Large-wavelength late Miocene thrusting in the North Alpine foreland: Implications for late orogenic processes

Samuel Mock[1], Christoph von Hagke[2], Fritz Schlunegger[1], István Dunkl[3], Marco Herwegh[1]

[1]Institute of Geological Sciences, University of Bern, Baltzerstrasse 1+3, 3012 Bern, Switzerland

[2]Institute of Geology and Palaeontology, RWTH Aachen University Wüllnerstrasse 2, 52056 Aachen, Germany

[3]Geoscience Center, Sedimentology and Environmental Geology, University of Göttingen Goldschmidtstrasse 3, 37077 Göttingen, Germany

Correspondence to: Samuel Mock (samuel.mock@geo.unibe.ch)

Abstract. ~~Additional to classical nappe tectonics, the Oligocene to mid-Miocene post-collisional evolution of the Central European Alps was characterized by vertically directed tectonics, with backthrusting along the Insubric Line and the subsequent uplift of the External Crystalline Massifs (ECMs). Thereafter, the orogen experienced axis-perpendicular growth when deformation propagated into its external parts. For the North Alpine foreland between Lake Geneva and Lake Constance, in the past, this has been kinematically and spatially linked to the uplift and exhumation of the ECMs. Based on apatite (U-Th-Sm)/He thermochronometry, we constrain thrusting in the Subalpine Molasse between 12-4 Ma, thus occurring coeval to main deformation in the Jura fold and thrust belt (FTB) and late stage exhumation of the ECMs. However, this pattern of tectonic activity is not restricted to areas which are bordered by ECMs, but is consistent along the northern front of the Alps between Geneva and Salzburg. Therefore, late Miocene foreland deformation is not necessarily a consequence of uplift and exhumation of the ECMs. While the local geometry of the Subalpine Molasse results from lateral variations of the mechanical stratigraphy of the foreland basin sediments, we suggest that the large-wavelength tectonic signal is the response to a shift in tectonic forces possibly caused by deep-seated geodynamic processes. This resulted in a change from dominantly vertical to horizontal tectonics and orogen-perpendicular growth of crustal thickening. We constrain the onset of this major tectonic change to ca. 12 Ma in the North Alpine foreland, resulting in thrusting and folding in the Subalpine Molasse west of Salzburg and in the Jura FTB until at least 4 Ma.~~

In this paper, we present new exhumation ages for the imbricated proximal Molasse, i.e. Subalpine Molasse, of the northern Central Alps. Based on apatite (U-Th-Sm)/He thermochronometry, we constrain thrust-driven exhumation in the Subalpine Molasse between 12-4 Ma. This occurs synchronously to main deformation in the adjacent Jura fold-and-thrust belt farther north and to late stage thrust-related exhumation of the basement massifs (i.e. External Crystalline Massifs) in the hinterland. Our results agree with other findings along the North Alpine foreland. While site-specific variations in the mechanical stratigraphy of the Molasse deposits influence the pattern of thrusting at the local scale, we observe that late Miocene thrusting is a large-wavelength feature occurring along the North Alpine foreland between Lake Geneva and Salzburg. The extent of this thrusting signal as well as the timing suggests that late Miocene thrusting in the North Alpine foreland coincides with the geometries and dynamics of the attached Central Alpine slab at depth. Interestingly, this implies that the slab geometry at depth

do not coincide with the boundary between Eastern and Central Alps as observed in the surface geology. Using this observation, we propose that thrusting in the Subalpine Molasse and consequently also late-stage thrust-related exhumation of the External Crystalline Massifs, as well as main deformation in the Jura fold-and-thrust belt are linked to changes of slab dynamics.

1 Introduction

Deep crustal processes and slab dynamics have been considered to ~~strongly~~ influence the evolution of mountain belts (e.g., Davies and von Blanckenburg, 1995; Molnar et al., 1993; Oncken et al., 2006). However, these deep-seated signals may be masked by tectonic forcing at upper crustal levels and by enhanced surface erosion related to climate change (e.g. Champagnac et al., 2007; Chemenda et al., 2000; Ganti et al., 2016; Whipple, 2009; Willett et al., 2006). In near surface crustal domains, it is thus challenging to isolate the exhumation signal related to slab dynamics. In this context, foreland basins offer suitable archives as they potentially bear information that allows to resolve the influence of deep-seated processes on mountain building. This is the case because these basins not only record signals that are related to surface dynamics such as changes of sediment fluxes and eustacy (e.g. Pippèrr and Reichenbacher, 2017; Sinclair and Allen, 1992~~). They~~), but they also preserve information on tectonic processes at the crustal and possibly mantle scales that operate at long timescales and large spatial wavelengths (e.g. DeCelles and Giles, 1996; Garefalakis and Schlunegger, 2018; Leary et al., 2016). The North Alpine foreland basin, or Molasse Basin, is particularly suited to constrain the geodynamic evolution of the collisional Alpine orogen because the history of this sedimentary trough has been well established through numerous magneto- and tectonostratigraphic (e.g. Burkhard and Sommaruga, 1998; Ganss and Schmidt-Thomé, 1953; Homewood et al., 1986; Kempf et al., 1999; Pfiffner, 1986; Schlunegger et al., 1996; Sinclair et al., 1991), seismic (Hinsch, 2013; Mock and Herwegh, 2017; Ortner et al., 2015; Sommaruga et al., 2012), and low-temperature thermochronological analyses (Cederbom et al., 2004, 2011; Gusterhuber et al., 2012; von Hagke et al., 2012, 2014b; Mazurek et al., 2006).

Studies from the forelands of the European Alps have shown that the most external parts of the orogen were incorporated into the orogenic wedge in Miocene times (e.g. Becker, 2000; Burkhard, 1990; von Hagke et al., 2012, 2014b; Hinsch, 2013; Ortner et al., 2015; Pfiffner, 1986; Schmid et al., 1996; Schönborn, 1992). In the case of the Swiss Molasse Basin, late Miocene deformation has been kinematically and spatially linked to the uplift and exhumation of the External Crystalline Massifs (ECMs~~)~~), which represent basement units derived from the subducting European plate~~, and~~. This late Miocene deformation phase was also linked to the main deformation in the Jura fold-and-thrust belt (FTB) situated at the northern margin of the Molasse Basin (Figs. 1 and 2; e.g. Boyer and Elliot, 1982; Burkhard, 1990; Burkhard and Sommaruga, 1998; von Hagke et al., 2014b; Laubscher, 1961, 1992; Mosar, 1999; Pfiffner, 1986; Sommaruga, 1999). The inferred linkages between the uplift of the ECMs, the imbrication of the proximal Molasse deposits, and the main deformation in the Jura FTB are mainly based on a classical scenario of ~~late stage~~ongoing continent-continent collision, where compressional wedge tectonics and shortening

result in crustal thickening of basement units in the hinterland and a propagation of the orogenic wedge towards the foreland, including imbricate thrusting (Pfiffner, 1986; Rosenberg and Berger, 2009; Schmid et al., 1996). ~~However, foreland propagation of deformation was not continuous as shown by structural, chronostratigraphic, and low-temperature thermochronological data, indicating that the Alpine thrust front advanced rather discontinuously during Miocene times~~

5 ~~(Beidinger and Decker, 2014; Burkhard and Sommaruga, 1998; von Hagke et al., 2014b; Ortner et al., 2015). In addition, the along strike partitioning of strain between the Jura FTB and the Subalpine Molasse has only incompletely been resolved so far. In the same sense~~

However, new studies from the Aar Massif of the Central Alps challenge this view. Based on geometric, kinematic, metamorphic, and geodynamic arguments, Herwegh et al. (2017, 2020) suggest for the exhumation of the eastern ECMs (Aar,

10 Mont Blanc, and Aiguilles Rouges Massifs) switches between 'horizontal' and 'vertical tectonics'. Note that the terms 'vertical' and 'horizontal tectonics' as used by Herwegh et al. (2017, 2020) are based on geometric and kinematic considerations, i.e. they imply a steeper or less steep orientation of the main faults along which strain is accommodated. Thus, in a compressional framework, these terms describe whether the vertical or the horizontal displacement components play the dominant role at a given point in time. Hence, the evolution of the Helvetic fold-and-thrust belt with the associated nappe

15 stacking represents an Oligocene stage of 'horizontal tectonics'. A major switch to 'vertical' tectonics occurred in early Miocene times when major parts of the Aar and Mont Blanc/Aiguilles Rouges Massifs experienced a strong vertical uplift component mainly along steep to sub-vertical reverse faults (Herwegh et al., 2017, 2020). This resulted in the differential uplift and doming of these eastern ECMs as well as a passive upward bulging of the entire nappe stack above. From a geodynamic point of view, (i) a retreating European slab, (ii) delamination of lower crust from the mantle, and (iii) a buoyancy-driven uplift

20 component within a compressional regime were suggested by aforementioned authors to be the driver for this 'vertical tectonic' forcing. It is important to stress that this 'vertical' exhumation component became dominant at a time when the up to only weakly thinned part of the buoyant former European passive continental margin entered the subduction channel. This stage of 'vertical tectonics' was followed by late Miocene 'horizontal tectonics', where en-bloc exhumation of the Aar Massif was accomplished through slip along shallow south-dipping basal thrust systems (Berger et al., 2017; Herwegh et al., 2017, 2020;

25 Mair et al., 2018). This scenario is described in a similar way for the Mont Blanc and Aiguilles Rouges Massifs for the same time interval (Burkhard and Sommaruga, 1998; Lacombe and Mouthereau, 2002; Bellahsen et al., 2014; Boutoux et al., 2016; Egli et al., 2017).

In addition to this ECM-related information, structural, chronostratigraphic, and low-temperature thermochronological data (Burkhard and Sommaruga, 1998; von Hagke et al., 2014b; Ortner et al., 2015) suggest that the Alpine deformation front

30 remained stationary within the Subalpine Molasse during the time of the inferred buoyancy-driven 'vertical tectonics'. The deformation then propagated to the Jura FTB during the late Miocene when the 'vertical tectonics' was superseded by the thrust-related exhumation in the Aar Massif (e.g. Burkhard and Sommaruga, 1998; von Hagke et al., 2012; Herwegh et al., 2020). The corresponding along-strike partitioning of strain between the Jura FTB and the Subalpine Molasse has, however,

only incompletely been resolved so far. Likewise, it has been unclear whether the amount of shortening within the Subalpine Molasse is consistent along strike, particularly with respect to the highly non-cylindrical architecture of the Alpine hinterland (Fig. 2).as well as the lentoid-shaped map appearance of the eastern ECMs (Fig. 2; Burkhard, 1990). However, this information is vital for understanding how deformation in the ECMs is potentially linked to foreland FTB tectonics. Accordingly, as a first

5 and major contribution of our paper, we aim at reconstructing the chronology and amount of shortening of the Molasse sequences during the late stage of Alpine orogeny since the mid-Miocene. Hereto, we build upon detailed andWe present new low-temperature thermochronological data from a key region in the western Subalpine Molasse and compare them with previously published data from farther east (von Hagke et al., 2012, 2014b). We combine this information with data from well-established work on the chronology, tectonics, and stratigraphy of the proximal foreland (thrusted Subalpine Molasse between

10 6.8° E (Lake Geneva) and 12.8° E (near Salzburg; e.g. Burkhard and Sommaruga, 1998; von Hagke et al., 2012, 2014b; Hinsch, 2013; Kempf et al., 1999; Ortner et al., 2015; Pfiffner, 1986; Schlunegger et al., 1997; and many others). We will relate these mechanisms) in order to better constrain the timing and spatial pattern of thrusting in the Subalpine Molasse. We will relate this to the history of shortening of the Jura FTB, and to Alpine tectonic events in an effort to identify possible relationships to possiblethe geodynamic forcing at thea larger scale.

15 Geological mapping of the Subalpine Molasse (e.g. Ganss and Schmidt-Thomé, 1953; Haldemann et al., 1980; Schlunegger et al., 2016; Weidmann et al., 1993; Zaugg et al., 2011) as well as stratigraphic work (e.g. Bachmann and Müller, 1992; Kempf et al., 1999; Lemcke, 1988; Schlunegger et al., 1993, 1997; Schlunegger and Kissling, 2015) has shown that the proximal basin border is characterized by large orogen-parallel lithologic variations where km-thick conglomerate suites with high mechanical strengths alternate with mudstones and sandstones with low at-yield conditions over lateral distances of a few kilometers. As

20 a consequence, the patterns of thrust faults and folds within the Subalpine Molasse change along-strike. In regions where the km-thick conglomerate packages are present, the geometry of the Subalpine Molasse is characterized by km-spaced thrust faults with a relatively large displacement.displacements on the In areas however, where the foreland mechanical stratigraphy mainly consists mostly of sandstone-mudstone alternations, the structural style is characterized by closely-spaced folds and thrust faults with possibly smaller displacements. (e.g. Kempf et al., 1999; Ortner et al., 2015; Schlunegger et al.,

25 1993, 19 We expect that these differences in mechanical stratigraphy leave a distinctan imprint on where strain iswas accommodated during late orogenic shortening. Therefore, as a related second contribution, we aim at exploring how lithological variations within the foreland basin, which were controlled by the paleogeographic conditions, contributed to the spatial distribution of late orogenic strain.

In summary, we present new low-temperature thermochronological data from a key region in the western Subalpine Molasse
30 and compare them with previously published data from farther east (von Hagke et al., 2012, 2014b). We combine this with tectono-sedimentological data along the thrusted Subalpine Molasse between 6.8° E (Lake Geneva) and 12.8° E (near Salzburg) in order to better constrain the timing and spatial pattern of thrusting in the Subalpine Molasse and the associated late-orogenic large-scale change from dominantly vertical to dominantly horizontal tectonics.

2 Geological and tectonic setting

2.1 The Central Alps

5 ~~We focus our study on the Central Alps because the inversion of the proximal basin part by imbricate tectonics during late Miocene times terminates near Salzburg (Fig. 1). This is also the region where the configuration of the lithospheric mantle slabs at depth changes along strike. Seismo~~Classically, the boundary (or transition) between the Central and the Eastern Alps has been located in eastern Switzerland. There, remnants of the Piemont-Ligurian Ocean separate units of European origin (Central and Western Alps) from thrust nappes that are part of the Adriatic continental plate (Figs. 1 and 2; Eastern Alps; Schmid et al., 2004). However, this surface observation is not reflected in the slab geometry at depth. Instead, seismo-tomography studies have disclosed that the subducting European slab beneath the Central Alps extends to the east until ca.

10 12.5° E, i.e. the area of Salzburg, ~~while~~whereas farther east, a segmentation of the slab structure is observed (Hetényi et al., 2018; Kästle et al., ~~2019~~2020; Lippitsch et al., 2003; Mitterbauer et al., 2011; Zhao et al., 2016; see further details in the discussion section). ~~Classically, the boundary (or transition) between the Central and the Eastern Alps has been located in eastern Switzerland where remnants of the Piemont-Ligurian Ocean separate units deriving from the former European passive margin (Central and Western Alps) from units deriving from the Adriatic Plate north of the Insubric Line (Figs. 1 and 2;~~

15 ~~Eastern Alps; Schmid et al., 2004). However,~~Similar to Rosenberg et al. (2018), we ~~place~~shift the boundary between the Central and Eastern Alps farther east. But instead of placing it at the Giudicarie-Brenner fault system (Rosenberg et al., 2018), we follow the argumentation given above, which is also advocated by Kissling and Schlunegger (2018), and place the Central-Eastern Alps transition where the current slab configuration changes at depth~~, following hereby a definition recently used by others (Kissling and Schlunegger, 2018; Rosenberg et al., 2018).~~. This is particularly important when the influence of

20 subduction mechanisms on the surface geology during the past few millions of years is ~~addressed~~considered, which is the scope upon discussing the results at the end of this paper. ~~We will~~In this study, we therefore focus ~~in this section~~ on the ~~geological~~Central Alps because late Miocene thrusting in the Subalpine Molasse terminates near Salzburg (Fig. 1; Beidinger and ~~tectonic setting~~Decker, 2014; Hinsch, 2013; Ortner et al., 2015), which spatially coincides with the aforementioned along-strike changes in the configuration of the ~~Central Alps, but~~lithospheric mantle slabs at depth. However, we will elaborate on

25 the influences of Eastern Alpine tectonic processes in the discussion part of this paper.

The Central Alps are situated almost entirely on top of the subducted Central European lithospheric slab (Figs. 2a and 2b; Schmid et al., ~~1996,~~2017), which steeply dips into the asthenospheric mantle as imaged by teleseismic tomography (Lippitsch et al., 2003). The ~~bivergent~~ orogen is the result of the Late Cretaceous to Eocene ~~ocean-continent~~ subduction of the oceanic part of the European plate under the Adriatic ~~plate and subsequent post~~continental plate post-35 Ma continent-continent

30 collision (e.g. Schmid et al., 1996). Subduction initially affected the European oceanic lithosphere, which was followed by subduction of the distal spur of the Iberian plate that became the Penninic thrust nappes. During the Eocene, subduction started to involve the distal and stretched European continental margin, (e.g. Cardello et al., 2019; Mosar et al., 1996; Stampfli and

Marchant, 1997). The subduction system then became clogged when the thick and buoyant European crust started to enter the subduction zone, which resulted inchannel. As a result, the subducted oceanic slab breakoffof the European plate supposedly broke off, which has been inferred from widespread plutonism ca. 32 Myr ago (Davies and von Blanckenburg, 1995). Slab unloading and basal accretion of crustal segments to the upper plate resulted in a period of fastthe rock and surface uplift,

5   whichgiving way to the incipient rise of the Alpine topography. Uplift was mainly accommodatedaccomplished through backthrusting along the Insubric Line (Hurford, 1986; Schmid et al., 1996). The signal of slab breakoff is), and was also manifested in the rapid build-up of topography and in the subsequent increase of sediment discharge into the Alpine foreland (Schlunegger and Castelltort, 2016; Sinclair, 1997). Recently, the idea of slab breakoff has been challenged and instead the volcanic and tectonic signal has been attributed to slab-steepening and consequently enhanced corner flow (Ji et al., 2019). At

10 20 Ma and therefore synchronous to the 'vertical' tectonic stage of the exhumation of the eastern ECMs, slip along the Simplon fault zone resulted in rapid exhumation of the Lepontine dome that is situated between the Aar Massif and the Insubric Line (Berger et al., 2011; Boston et al., 2017; Todd and Engi, 1997). However, we do not consider that tectonic exhumation of the Lepontine had an influence on the history of thrusting in the proximal Molasse basin since there is no mechanical link (Schmid et al., 1996). Therefore, in the following, the deformation along the Simplon fault zone will not be considered.

15 During the Oligocene, Europe-derived sedimentary units were sheared off from their substratum and emplaced to the north over a distance of several tens of kilometers thereby forming the present-day Helvetic cover nappes (Pfiffner, 2011, and references therein). Ongoing orogenyconvergence resulted in delamination of lower European crustal segments from the lithospheric mantle (Fry et al., 2010),.). This mechanism eventually inducingresulted in buoyancy-driven subvertical uplift (sub-vertical tectonics)uplift of the thickened crust (Kissling and Schlunegger, 2018) along steeply dipping shear zones and in

20 exhumation of the ECMs ca. 20 Myr ago (Fig. 2a; e.g. Egli et al., 2017; Glotzbach et al., 2011; Herwegh et al., 2017, in press2020). Farther east, between the Aar Massif and the Brenner Fault (a segment, which we here consider as the eastern Central Alps), such Europe-derived crustal blocks are not exposed at the surface. East of the Brenner Fault (Fig. 1), northward indentation of the Dolomite indenter resulted in eastward-directed lateral extrusion of crustal blocks, which started in early Miocene times (Frisch et al., 1998; Handy et al., 2015; Ratschbacher et al., 1991). AssociatedThis process was associated with

25 this was the exhumation of the Tauern Window, which was accomplished by upward folding and erosion of the nappe pile, and by normal faulting along its bounding low-angle normal faults (see Rosenberg et al., 20 8)

The late stageLate stages in the evolution of the Central Alps isare dominated by orogen-perpendicular growth due towhen the propagation of deformation to its front on either side of the Alps propagated to the external parts, i.e., toresulting in the Molasse Basin anddevelopment of the Jura fold-and-thrust belt (FTB) and the Subalpine Molasse in the north, and to the Southern Alps

30 inon the southsouthern side of the Alps (Figs. 1 and 2; Burkhard, 1990; Caputo et al., 2010; Castellarin and Cantelli, 2000; Nussbaum, 2000; Pfiffner, 1986; Schmid et al., 1996; Schönborn, 1992), thereby marking a change from dominantly vertical to horizontal tectonics (Schlunegger and Simpson, 2002). In the Southern Alps, fold and thrust belts evolved from late

~~Oligocene times on onwards, but the largest amounts of shortening occurred after ca. 15 Ma (Caputo et al., 2010; Castellarin and Cantelli, 2000; Schmid et al., 1996; Schönborn, 1992).)~~.

2.2 The Molasse Basin

2.2.1 Structures and tectonic evolution

5   The Molasse Basin of the North Alpine foreland, which contains ~~erosional products~~deposits derived from the progressive erosion of the evolving Alps since 32 Ma (Sinclair et al., 1991), ~~is~~can tectonically be subdivided into three parts: (i) The Plateau Molasse is the gently folded part of the basin, which evolved into a wedge-top basin (e.g. Willett and Schlunegger, 2010) during late Miocene main Jura FTB deformation, when it became detached above a main décollement zone within the Triassic evaporites. (ii) To the east, with the Triassic evaporites diminishing and the Jura FTB tapering off, the basin gradually changes

10 into a non-detached configuration, the For[clan]d Molasse. (e.g. Berge and Veal, 2005; Ortner et al., 2015; Pfiffner, 1986). (iii) At the southern, proximal basin border, the Subalpine Molasse extends continuously as a narrow band of imbricates from south of Geneva to Salzburg, where it disappears ~~below~~beneath Helvetic and Penninic units before it emerges again in upper Austria. In this contribution we mainly focus on the Subalpine Molasse between Lake Geneva and Salzburg, i.e. the part of the fold-thrust belt ~~that can~~where the tectonic processes may be ~~considered being~~ associated with the subduction of the European

15 lithospheric slab of the Central Alps.

The Subalpine Molasse consists of south-dipping imbricated thrust sheets ~~and in~~. In large parts and predominantly northeast of the Lake Thun area, the structures of the Subalpine Molasse also include the north-dipping backthrusts ~~forming~~that form a triangle zone at the transition to the Plateau and Foreland Molasse (Fig. 2; Berge and Veal, 2005; Fuchs, 1976; Müller et al., 1988; Ortner et al., 2015; Schuller et al., 2015; Sommaruga et al., 2012). The Subalpine Molasse started to become incorporated

20 into the orogenic wedge shortly after deposition in Oligocene times (Hinsch, 2013; Kempf et al., 1999; Pfiffner, 1986). After ca. 20 Ma, contemporaneously with the development of the frontal triangle zone, the northern Alpine thrust front remained stationary in the area of the Subalpine Molasse (Burkhard and Sommaruga, 1998; von Hagke et al., 2014b; Ortner et al., 2015). It was not until ca. 12 Ma when parts of the deformation in the western Molasse Basin (i.e. the Molasse west of Lake Constance) propagated along a basal décollement zone within the Triassic evaporites into the thin-skinned Jura FTB (Becker, 2000;

25 Burkhard and Sommaruga, 1998; Laubscher, 1961; Philippe et al., 1996), although already in the late Oligocene some deformation occurred in the area of ~~the~~ today's Jura FTB (Aubert, 1958; Liniger, 1967). Hence, during the late Miocene, the Molasse Basin experienced along-strike changes in tectonic style and locus of deformation. While sediment accumulation in the eastern Molasse Basin (i.e. here the Foreland Molasse between Lake Constance and Salzburg) occurred still in a foredeep setting, the western part evolved at this stage into a wedge-top basin (i.e. Plateau Molasse; Willett and Schlunegger, 2010~~), as~~

30 ~~it was detached above the basal décollement zone.~~). Both, the evaporite basal décollement and the thrusts of the Subalpine Molasse are considered to root below and in the ECMs. Accordingly, they were kinematically linked to the late Miocene exhumation of the ECMs (Fig. 2a; e.g. Burkhard, 1990), which was driven at that time by north-directed thrusting along

shallow dipping faults (Herwegh et al., 2017, in press2020), thereby causing a phase of accelerated exhumation at ca. 10 Ma (Fox et al. 2016; Glotzbach et al., 2010; Valla et al., 2012; Vernon et al., 2009; Weisenberger et al., 2012). Based on stratigraphic data, Haus (1935) inferred already in 1935 that the Subalpine Molasse of Central Switzerland was subject to major thrusting in late Miocene times. Recently, studies have revisited this topic and documented that the Subalpine Molasse

5 was subject to break-back thrusting between ca. 13 Ma and 4 Ma (von Hagke et al., 2012, 2014b; Ortner et al., 2015; Schuller et al., 2015), which was thus coeval to folding and thrusting in the Jura FTB. We note that late Miocene thrusting is not recorded forin the Subalpine Molasse east of Salzburg (Beidinger and Decker, 2014; Hinsch, 2013; Ortner et al., 2015), i.e. where the deep slab configuration of the Eastern Alps is present.).

After 10 Ma, but possibly as late as 5 Ma, the entire Molasse Basin was uplifted, resulting in basin-scale erosion (Baran et al.,

10 2014; Cederbom et al., 2004, 2011; Genser et al., 2007; Gusterhuber et al., 2012; von Hagke et al., 2012; Mazurek et al., 2006; Schlunegger and Mosar, 2011; Zweigel et al., 1998). Since 5 Ma, compressional thin-skinned tectonics in the wedge-top part of the basin and the Jura FTB are superseded by thick-skinned tectonics (Giamboni et al., 2004; Guellec et al., 1990; Madritsch et al., 2008; Mock and Herwegh, 2017; Mosar, 1999; Philippe et al., 1996; Ustaszewski and Schmid, 2007).

15 2.2.2 Stratigraphic development

The clastic infill of the Oligocene to Miocene peripheral Molasse Basin consists of the eroded sediments of the evolving Alps, and in the northern parts partly of material shed from the Black Forest and the Bohemian Massif. Accommodation space was formed through subsidence, classically related to flexural bending of the European plate in response to the combined effect of subsurface slab loading and topographic loading of the advancing Alpine thrust wedge during Paleogene and Neogene times

20 (Allen et al., 1991; Burkhard and Sommaruga, 1998; Karner and Watts, 1983; Pfiffner, 1986; Zweigel et al., 1998). For the Central Alps, this view has recently been challenged by Schlunegger and Kissling (2015), who favor a slab rollback mechanism, to explain foreland plate flexuringflexure and accommodation space formation. In this scenario, slab rollback is driven by the interplay between vertically-directed slab loads exerted by the subducted European lithospheric mantle and buoyancy-driven crustal delamination (Kissling and Schlunegger, 2018).

25 In the Swiss part of the basin, the Molasse sediments form two regressive and coarsening-upward megasequences (Homewood et al., 1986; Kuhlemann and Kempf, 2002; Schlunegger et al., 2007). The first megasequence describes the transition from Rupelian (ca. pre-30 Ma) sedimentation in underfilled conditions to Chattian-Aquitanian (ca. 28-20 Ma) sedimentation when the basin was overfilled. The Burdigalian (ca. 20-17 Ma) and post-Burdigalian (ca. post-17 Ma) stratigraphic records then chronicle the second megasequence during filled to overfilled conditions (Sinclair and Allen, 1992). West of ca. 11° E, large

30 alluvial megafans developed at the mountain front during the overfilled stage of the basin (Frisch et al., 1998; Kuhlemann and Kempf, 2002; Ortner et al., 2015). In their cores, close to the apex, large and km-thick conglomerate bodiessequences were deposited, while at the margins, the sedimentation was mainly sand- and mudstone dominated. At the proximal basin border,

numerous locally-derived bajada fans discharged sediments into the foreland and thus further contributed to the high along-strike stratigraphic variability at the proximal basin border (Kempf et al., 1999; Schlunegger et al., 1997; Spiegel et al., 2001). Farther east, the Molasse Basin prevailed in an underfilled stage ~~during this time~~until at least 17 Ma, when sedimentation of sandstones and marls occurred under brackish to shallow marine conditions (Hinsch, 2013; Kuhlemann and Kempf, 2002;

5 Lemcke, 1988; Ortner et al., 2015). Large alluvial fans are missing due to the channelizing effect of the paleo-Inn river, which transported the erosional detritus effectively farther to the east (Frisch et al., 1998; Kuhlemann and Kempf, 2002). For more details on the laterally varying stratigraphy, including Wheeler diagrams, the reader is referred to Kempf et al. (1999), Schlunegger et al. (1997), and Schlunegger and Norton (2013) as well as Hinsch (2013), Kuhlemann and Kempf (2002), Lemcke (1988), and Ortner et al. (2015) for the Molasse Basin west and east of Lake Constance, respectively.

10 **3 Methods**

3.1 ~~Sample~~Selection of sample sites and litho-tectonic architecture

We consider the Lake Thun region as a key area for the understanding of Subalpine Molasse tectonics for the following reasons:

(i)   With the Aar Massif being one of the best studied ECM in the Alps in terms of its Alpine tectonic evolution and geodynamic significance, information on the history of thrusting of the Subalpine Molasse in front of the Aar

15   Massif is of great importance if the scope lies on reconstructing the post-collisional tectonic evolution of the Central Alps.

(ii)   The thickness of the basal décollement zone within the Mesozoic cover sediments below the Molasse Basin decreases significantly west of ca. 7° E (Landesgeologie, 2017; Mock and Herwegh, 2017; Sommaruga et al., 2012; Sommaruga et al., 2017). Hence, the Lake Thun area is located in an ideal place where we can expect the

20   eastward transition from the detached Plateau Molasse to the non-detached Foreland Molasse.

(iii)   While east of the Lake Thun area, the frontal part of the Subalpine Molasse is often delineated by a backthrust and a triangle zone, this feature is largely missing farther west, where predominantly northwestward imbricate thrusting occurs.

We collected ~~13~~12 samples across the Subalpine Molasse east and west of Lake Thun for apatite (U-Th-Sm)/He (AHe) dating

25 (Fig. 3). The northernmost samples represent coarse-grained Burdigalian sandstones of the Plateau Molasse. Further to the southwest, we sampled Chattian-Aquitanian and Rupelian sandstones within the Subalpine Molasse. Samples have been collected in the hanging- and footwalls of the individual thrusts (Fig. 3). To control the depositional age of the sediments, samples were taken in the vicinity of sites with known mammal ages and magneto-polarity based chronologies (Schlunegger et al., 1996; Strunck and Matter, 2002) wherever possible.

~~In the sampling area, mapping shows that the litho-tectonic architecture of the Subalpine Molasse contrasts between both sides of Lake Thun (Fig. 3). On the eastern side, the basin is made up of amalgamated conglomerates and a relatively large spacing between the major thrust faults, while the tectonic style of the Subalpine Molasse to the west of Lake Thun is characterized by more evenly distributed thrust sheets made up of alternated sandstone and mudstone beds. The same pattern can be found~~

5 ~~along strike where the distribution pattern of conglomerates, sandstones, and mudstones tends to condition the location and the spacing of thrust faults.~~ In order to test the influence of along-strike changes in the mechanical stratigraphy of the Subalpine Molasse on the thrusting pattern, wWe ~~thus~~ compiled more details about the geological architecture of the proximal Molasse from published geological maps (Landesgeologie, 2005) and use available tectonic sections (Ortner et al., 2015; Sommaruga et al., 2012) to illustrate the related tectonic style.

10 **3.2 (U-Th-Sm)/He (AHe) thermochronology and thermal modeling**

We determined the most recent exhumation history of the Subalpine Molasse of the Lake Thun region through AHe dating. This method is based on the α-decay of ^{238}U, ^{235}U, ^{232}Th and ^{147}Sm isotopes, and the retention of its radiogenic product ^{4}He in the crystal lattice below a certain temperature (e.g., Farley, 2002). Diffusive loss of ^{4}He in the lattice depends on the grain size, shape, chemical composition, distribution of the mother isotopes, radiation damage density, as well as the time-temperature

15 evolution of the crystal (Farley, 2002; Wolf et al., 1996). Consequently, AHe ages can provide estimates about the time when the mineral passed through the diffusion-sensitive temperature interval between ca. 80°C and 40°C (Wolf et al., 1996), which is referred to as the partial retention zone (PRZ). Hence, this ~~technology~~method allows constraining the tectono-thermal history of the studied rocks in the uppermost few kilometers of Earth's crust. Detrital apatite grains deposited in sedimentary basins primarily carry a cooling history of the hinterland at the time of erosion. Subsequent burial due to sedimentation or tectonic

20 loading may reheat the detrital grains to temperatures above the closure temperature, thereby resetting the chronometer. Subsequent exhumation will chronicle the basin's exhumation, whereas grains that have not been reset during the basin's burial history still carry a signal of older cooling events. Consequently, the relation between cooling age and stratigraphic age may provide estimates on the burial as well as the exhumation history (e.g., Reiners and Brandon, 2006).

We used a combination of standard techniques for the separation of apatite minerals, which particularly includes

25 electrodynamic disaggregation, and magnetic and heavy liquid separation. Single crystals were handpicked under a binocular and checked for inclusions and imperfections under an optical microscope with cross-polarized light (more information on the mineral separation techniques and picking criteria are given in Text ~~A1~~S1 in the supplementary material). Helium extraction and measurement of parent isotope contents has been conducted at the GÖochron laboratories of University of Göttingen. Raw ages were corrected for α-ejection (Table 1). We measured four to eight single grain ages per sample and calculated average

30 ages using the unweighted arithmetic mean for completely reset samples. We excluded single grain ages for subsequent geological interpretation based on the following criteria (Table 1): (i) high analytical errors (>10%), (ii) very low U-content (<10 ppm), (iii) a substantial amount of He on the first re-extract (>4%), or erroneous old ages stemming most likely from U-

Th rich mineral inclusions which produce parentless He. For the latter case, we plotted the He content versus the present-day He production rate in order to detect these ages (for details see Vermeesch, 2008).

We constrained the thermal histories of the sampled sediments (Fig. 4) by modeling of the AHe age data with the HeFTy software (Ketcham, 2005). We gave the algorithm a ~~maximum~~high degree of freedom. ~~Model~~ by using only a few modeling constraints ~~included~~: the age of sedimentation, the paleo-temperature (Mosbrugger et al., 2005), the present-day annual average temperature, and maximum post-depositional heating rates inferred from maximum sedimentation rates (Schlunegger and Norton, 2015) and a paleo-geothermal gradient of 28°C/km (Schegg and Leu, 1998).

4 Results

4.1 AHe age data

Samples SM-7 and SM-16 from the Plateau Molasse show a wide spread in AHe ages, indicating a partially exhumed fossil PRZ. Hence, they did not experience enough post-depositional heating for a full reset of the thermochronometer (Fig. 3b and Table 1). All other samples show single grain ages ~~reproducing~~which plot within error for each sample. Ages are significantly younger than the corresponding depositional ages and are thus considered to represent completely reset ages (fully exhumed fossil PRZ), hence inferring substantial post-depositional burial and heating.

Average ages for completely reset samples range from 6.0 ± 0.4 Ma to 10.8 ± 0.6 Ma (Fig. 3b and Table 1). All samples from the Subalpine Molasse show post-depositional burial and heating to >60°C (Fig. 4). Sample SM-7 from the Plateau Molasse did not experience enough post-depositional heating to fully reset the thermochronometer (Fig. 4). Thermal modeling supports the young exhumation of the Subalpine Molasse between 12 Ma and 5 Ma (Fig. 4). The thermal histories of SM-7 and SM-13 indicate an exhumation signal of the Plateau Molasse at ca. 10 Ma.

Samples SM-8, SM-11 and SM-15 were collected from the same tectonic sliver (Figs. 3a and 5), and corresponding average ages of 6.0 ± 0.4 Ma, 6.6 ± 0.4 Ma and 6.1 ± 0.4 Ma ~~reproduce~~group well within their margins of error. A jump ~~of~~in average ages occurs across the thrust to the adjacent tectonic slivers and the Plateau Molasse in the north, where samples SM-12, SM-13, and SM-14 yield average ages of 9.2 ± 1 Ma, 8.9 ± 0.7 Ma, and 10.8 ± 0.6 Ma, respectively, thus also ~~reproducing~~grouping within their margins of error. This pattern is also reproduced by the modeled thermal histories, where a jump in exhumation ages across tectonic boundaries is recognized (Fig. 4). In the western area, the average ages do not show such a close correlation with the tectonic position (Figs. 3a and 5). However, the thermal models for samples SM-5 and SM-6 indicate younger cooling than for samples SM-4 and SM-7 (Fig. 4), thus suggesting a tectonic control on exhumation.

4.2 Litho-tectonic architecture of the Lake Thun area

In the sampling area, mapping shows that the litho-tectonic architecture of the Subalpine Molasse contrasts between both sides of Lake Thun (Fig. 3). On the eastern side, the basin is generally made up of amalgamated conglomerates which are cut from west to east by two narrow sand- and mudstone dominated bands. The south-dipping thrust north of the Falkenfluh anticline

5 as well as the three tightly spaced thrusts further south all emerge along these mechanically weaker bands (Fig. 3a). In between these thrust domains, we observe large tectonic slices made up of mechanically strong conglomerates of Burdigalian (north) and Chattian-Aquitanian age (south). The latter is bordered to the north by three thrusts for which we can infer from cross-cutting relationships in map view a break-back sequence of thrusting (i.e. out-of-sequence; Fig. 3a). To the south, across a south-dipping thrust, Rupelian sand- and mudstones crop out. West of the Aare valley, conglomerates are largely absent and

10 the stratigraphy is sand- and mudstone dominated. Compared to the Subalpine Molasse east of the Aare valley, the FTB is much narrower, thrusts are more evenly distributed, and the tectonic slices are less wide (Fig. 3). Across the whole area we can see a clear correlation between the distribution of mechanically weak sand- and mudstones and the location and alignment of thrust faults. The subsurface continuation of the thrusts has been inferred from seismic interpretation (for more details see Mock and Herwegh, 2017). It suggests that the thrusts merge in a detachment level at a depth of ca. 2km (Fig. 3b). The type

15 of lithology of the detachment remains however unknown, since the poor signal-to-noise ratio of the seismic images does not allow a clear distinction with this respect. Due to the lack of subsurface data further south it also remains speculative on how the structures extend southward. As indicated in the sections (Fig. 3b), it is though likely that the thrusts root within the Rupelian sand- and mudstones at the base of the Molasse sequence on top of the Mesozoic cover sediments. In summary, we observe pronounced differences both in the mechanical stratigraphy as well as in the structural configuration of the Subalpine

20 Molasse west and east of the Aare valley. We discuss this in detail in section 5.1 below.

4.3~~2~~ Late Miocene shortening estimates

Based on published restored cross-sections (Burkhard and Sommaruga, 1998; von Hagke et al., 2014b; Ortner et al., 2015), retro-deformed and balanced palinspastic maps (Philippe et al., 1996), thermochronological age data (von Hagke et al., 2012, 2014b), and own cross-section restorations, (see Text S2 and Figure S1 in the supplementary material), we estimated the

25 amount of late Miocene horizontal shortening of the Subalpine Molasse and the Jura FTB from Lake Geneva to Salzburg (Fig. 6b). Post-12 Ma horizontal shortening in the Jura FTB decreases from a maximum of ca. 32 km in the west to 0 km at the eastern tip (Philippe et al., 1996). Contrariwise, minimum horizontal shortening in the Subalpine Molasse increases from ca. 10 km in the west (Lake Geneva) to ca. 20 km farther east (Lake Constance), before decreasing again to below 1 km in the area near Salzburg (Beidinger and Decker, 2014; Burkhard and Sommaruga, 1998; von Hagke et al., 2012, 2014b; Hinsch,

30 2013; Ortner et al., 2015). These values do not account for shortening taken up by the frontal triangle zone between ca. 20 Ma and 12 Ma (von Hagke et al., 2014b; Kempf et al., 1999; Ortner et al., 2015). ~~Despite the uncertainty in the~~ We acknowledge that shortening estimates ~~within~~for the Subalpine Molasse are subject to uncertainties (Burkhard and Sommaruga, 1998; von

Hagke and Malz, 2018; Ortner et al., 2015), and likely represent minimum estimates due to: (i) the unconstrained large parts of proximal Subalpine Molasse, which are hidden below the frontal thrusts of the Helvetic nappes and Penninic Klippen units, and (ii) the non-preservation of the hanging-wall cut-offs of individual thrust sheets. Despite these uncertainties, we observe that late Miocene cumulative shortening of the Subalpine Molasse and the Jura FTB decreases constantlyslightly from the west

5   to the east from >30 km near Geneva to 20 km near Lake Constance, before finallyrapidly decreasing to <1 km nearbetween ca. 10.5° E and Salzburg (12.8° E; Fig. 6b). It is thus noteworthy that the along-strike variation in late Miocene shortening in the foreland does not correlate with the peaks of high-uplift domains ofseem to reflect the different levels of exhumed European basement units (i.e. ECMs) in the hinterland (Fig. 6c).

5 Discussion

10   **5.1 Downscaling: Local-scale stratigraphic architecture conditioning the pattern of strain releaseaccommodation**

In the sampling area, mapping discloses along-strike differences in the litho-tectonic architecture of the Subalpine Molasse (Fig. 3). The sediments are thrusted northwestward along SW-NE striking thrusts. East of the Aare valley, a back-thrustbackthrust emerges to the surface and forms a frontal triangle zone (Figs. 3 and 5), a structure which is also known from parts of the Subalpine Molasse farther east (Fig. 7; e.g. Berge and Veal 2005; Müller et al. 1988; Schuller et al. 2015;

15   Sommaruga et al. 2012; Stäuble and Pfiffner 1991, Ortner et al. 2015). The Aare valley, running across the study area, is characterized by a low relief and is filled by >100 m-thick Quaternary deposits (Fig. 5; Dürst Stucki et al., 2010). Accordingly, the structural configuration of this part of the study area is only poorly resolved. However, the structures of the Subalpine Molasse change abruptly across the Aare valley (Figs. 3 and 5), as has been described by many authors (Beck, 1945; Blau, 1966; Haus, 1937; Pfiffner, 2011; Rutsch, 1947; Vollmayr, 1992). Based on this observation and under the consideration of

20   available interpreted reflection seismic lines, the presence of a possible syn-thrusting strike-slip fault zone running along the valley axis has been proposed (Mock and Herwegh, 2017; Pfiffner, 2011; Vollmayr, 1992). The presence of such a fault is, however, speculative due to the low resolution of the seismic data. The latter stems from (i) the thick Quaternary cover resulting in a very poor signal-to-noise ratio and (ii) the poorly resolved Molasse strata as a result of the frequency, which was chosen in order to optimize for the targeted Mesozoic horizons below (Mock and Herwegh, 2017). An alternative explanation for the

25   sudden along-strike change in the tectonic architecture has first been proposed by Rutsch (1947). He reported that the change from a mainly conglomeratic (east) to a sand- and mudstone dominated (west) lithofacies coincides with an increase in the folding intensity along the frontmost anticline (Falkenfluh anticline; Fig. 3a). Indeed, while conglomerates are the dominant lithofacies in the eastern part of the study area, they are vastly absent west of the Aare valley, where mainly alternating sequences of sandstones and mudstones are outcropping (Figs. 3 and 7; Landesgeologie, 2005). This difference in mechanical

30   stratigraphy east and west of the Aare valley is probably a result of an asymmetric dispersal system with a distinct northeastward direction of sediment discharge (Schlunegger and Norton, 2015). The distribution of mechanically different

lithologies seems to control the pattern of ~~strain release (i.e.~~ thrusting ~~pattern).~~. While east of the Aare valley, the mechanically stronger thick conglomeratic sequences deform en-bloc and thrusts are concentrated in narrow bands following mechanically weak zones of sand- and mudstones, strain is ~~released~~accommodated in a much more distributed pattern along more closely spaced thrusts in the western part of the study area~~.~~ (Fig. 3). The pronounced mechanical contrast between conglomerates and

5 sand-/mudstones leads to en-bloc thrusting of the large tectonic slice made up of amalgamated conglomerates east of the Aare valley, and it is also manifested in well-defined and constant AHe ages of ca. ~~6 Ma (Figs. 3 and 5). AHe ages west of the Aare valley, however, chronicle a more evenly distributed deformation and exhumation pattern, which is most likely conditioned and thus controlled by the low mechanical contrast of the involved lithologies.~~6 Ma within this tectonic slice (samples SM-8, SM-11, and SM-15; Figs. 3 and 5).

10 The observation that along-strike variations in the stratigraphic architecture lead to complex patterns of strain ~~release~~accommodation is not unique to our ~~sample~~study area, but can be also made ~~also~~ at the Mont Pèlerin, the Rigi, or the Hörnli in western, central, and eastern Switzerland, respectively (Fig. 7). ~~In particular,~~Salients seem to occur at the apex of former alluvial megafan depositional systems, while recesses are observed in regions in between these large dispersal systems, where thick conglomerate sequences are missing. The lithological control on the strain ~~release~~accommodation and exhumation

15 pattern is particularly well observed in the Rigi area (profile 3 in Fig. 7; Sommaruga et al., 2012). The thick conglomerate sequence of the Rigi thrust sheet was (re-)activated en-bloc at ca. 5 Ma, while the adjacent sand- and mudstone dominated part to the north experienced a period of thrusting at ca. 9 Ma along evenly spaced faults (von Hagke et al., 2012). Similar dependencies between the style of deformation and lateral changes in lithology have also been described for the Subalpine Molasse in Bavaria and western Austria (for detailed information see Ortner et al., 2015), as well as for the basal detachments

20 of the Subalpine Molasse and the Jura FTB (von Hagke et al., 2014a). While large alluvial fans ~~deposited~~formed thick conglomerate-sandstone sequences in western Bavaria, brackish to shallow marine conditions prevailed farther east where marls and sandstones were deposited (Frisch et al., 1998; Kuhlemann and Kempf, 2002). This lateral change of the Molasse's mechanical stratigraphy has been described to have a direct influence on the deformation style of the Subalpine Molasse (Ortner et al., 2015). While stacks of tectonic horse structures and a pronounced triangle zone developed in western Bavaria,

25 the deformation style changes to buckle folding farther east, which decreases in amplitude and the triangle zone disappears (a detailed description is provided in Ortner et al., 2015). Numerical models of syntectonic sedimentation support that sediments shed on an evolving FTB strongly control its geometry, and may include formation of backthrusts (e.g. Fillon et al., 2013).

5.2 ~~Upscaling:~~ Implications for late orogenic processes

5.2.1 The link to exhumation of the External Crystalline Massifs

30 Classically, thrusting in the Jura FTB and the Subalpine Molasse between Lake Geneva and Lake Constance has been kinematically and spatio-temporally related to the uplift and exhumation of the ECMs, and to the propagation of the deformation front towards the foreland (Burkhard, 1990; Burkhard and Sommaruga, 1998; Pfiffner et al., 1997). The Aar, and

possibly also the Mont Blanc, and Aiguilles Rouges Massifs were exhumed in early to mid-Miocene times during a stage of buoyancy-driven differential uplift along sub-vertical reverse faults ('vertical tectonics'; Herwegh et al., 2017, 2020). This stage of 'vertical tectonics' was followed by late Miocene en-bloc exhumation along a series of shallow southwest-dipping basal thrusts at the massif's northwestern front (Egli et al., 2017; Herwegh et al., 2017, 2020;). It is during this late (ca. post-

5 13 Ma) thrusting-dominated phase (i.e. 'horizontal tectonics') when deformation was translated northward into the Alpine foreland. In the non-detached part of the North Alpine foreland, thrusting of the proximal Molasse occurred. Far-field stress transferred into the foreland, induced the reactivation of Paleozoic structures (Egli et al., 2016). In the western North Alpine foreland, large-scale strain partitioning occurred when deformation propagated 50-90 km to the north forming the Jura FTB, while at the same time imbricates of Subalpine Molasse were thrusted northward (e.g. Becker, 2000; Burkhard, 1990; Burkhard

10 and Sommaruga, 1998; von Hagke et al., 2012).

However, it has also been reported that the proximal foreland basin east of the easternmost ECM, i.e., the Aar Massif, has been subject to post-12 Ma thrusting and horizontal shortening (Figs. 6a and 6b; Ortner et al., 2015). Our AHe age data from the Subalpine Molasse (Figs. 3, 4, and 5) fit with AHe ages farther east (von Hagke et al., 2012, 2014b) and chronicle a period of thrusting and exhumation of the Subalpine Molasse between 12 Ma and 4 Ma (Fig. 6a). This occurred ~~coeval~~coevally with the

15 main deformation phase in the Jura FTB, which lasted from ca. 12-4 Ma (e.g. Becker, 2000). Similar ages constrained from geological and seismic interpretation, and observations of growth strata in the youngest preserved sediments have been reported for the Subalpine Molasse between Lake Constance and Salzburg (Fig. 6a; Ortner et al., 2015). ~~Based on stratigraphic data, Haus (1935) inferred already in 1935 that~~ Late Miocene thrusting in the Subalpine Molasse of Central Switzerland ~~was subject to major thrusting in late Miocene times.~~ has also been inferred from stratigraphic data (Haus, 1935). Since the youngest

20 AHe ages are ~~associated with~~recorded from the internal tectonic slices of the Subalpine Molasse (Figs. 3, 4, and 5), we can infer the occurrence of break-back thrusting, a characteristic feature, which has been confirmed so far along the Subalpine Molasse between Bern and Salzburg based on thermochronological data and cross section restorations (von Hagke et al., 2012, 2014b; Ortner et al., 2015; Schuller et al., 2015), but has been locally argued for as early as the 1930s (Haus, 1935, 1937). The break-back thrusts are supposedly younger than the development of the frontal triangle zone, which formed the active northern

25 deformation front from ca. 20-12 Ma (von Hagke et al., 2014b; Ortner et al., 2015). Furthermore, our AHe ages from the Plateau Molasse record a partially exhumed PRZ (Figs. 3, 4, and 5) and thus corroborate the occurrence of substantial exhumation of the flat-lying Plateau and Foreland Molasse (Cederbom et al., 2011; Genser et al., 2007; Gusterhuber et al., 2012; von Hagke et al., 2012; Zweigel et al., 1998), indicating a large wavelength exhumation signal across the entire basin. ~~Because the tectonically driven exhumation signal between 12 Ma and 4 Ma is not unique to the forelands of the ECMs and~~

30 ~~late Miocene shortening estimates in the North Alpine foreland do not correlate spatially with the high-uplift domains of the ECMs (Fig. 6), we suggest that although kinematically linked, the late Miocene foreland deformation is not a consequence of uplift and exhumation of the ECMs.~~

Although foreland deformation is kinematically linked to the late phase of thrust-dominated exhumation of the ECMs ('horizontal tectonics'; Herwegh et al., 2017, 2020), the occurrence of late Miocene thrusting in the foreland is not restricted to the areas in front of the ECMs, and the along-strike variation in horizontal shortening does not seem to reflect the different levels of exhumed basement blocks (i.e. ECMs) in the hinterland (Fig. 6). Based on the observations of a continuous down-going European slab in combination with the extent of the Subalpine Molasse, we suggest that late Miocene thrusting is a large wavelength feature which occurs along the entire northern Central Alps encompassing both the ECMs and the foreland (i.e. Subalpine Molasse and Jura FTB; Fig. 8c). This follows an early to mid-Miocene stage, which was characterized by the sub-vertical extrusion of the eastern ECMs and a stationary deformation front in the Subalpine Molasse. Hence, along the northern Central Alps, the mid-late Miocene boundary marks the transition from an inferred buoyancy-driven regime with the sub-vertical rise of the eastern ECMs ('vertical tectonics'; Herwegh et al., 2017, 2020) to a large-scale thrust-dominated regime ('horizontal tectonics'), thereafter.

5.2.2 Possible link to geodynamic processes beneath the core of the Central Alps

During mid- to late Miocene times, the Central Alps underwent a major change from dominantly vertical to horizontal tectonics. This is also witnessed by the supersession of the vertical extrusion of the ECMs by north-directed thrusting along shallow SE-dipping shear zones (Fig. 8c; Herwegh et al., 2017, in press). In the western North Alpine foreland, large-scale strain partitioning occurred when deformation propagated 50-90 km to the north into the Jura FTB (Becker, 2000) while at the same time the Subalpine Molasse experienced break-back thrusting and thrust reactivation along the entire segment of the Alps between Lake Geneva and Salzburg (Figs. 6a and 8c). The occurrence of late Miocene thrusting has also been reported for the foreland of the Western Alps (Schwartz et al., 2017). In the Southern Alps, deformation propagated ca. 50 km southward between ca. 15 Ma and 7 Ma (Schmid et al., 1996; Schönborn, 1992).

This rapid change from pre-12 Ma vertical tectonics in the core of the Alps (Herwegh et al., 2017; Hurford, 1986; Schmid et al., 1996This transition from pre-12 Ma buoyancy-driven 'vertical tectonics' (Herwegh et al., 2017, 2020), with the triangle zone in the Subalpine Molasse acting as a stationary deformation front from ca. 20-12 Ma (von Hagke et al., 2014b; Ortner et al., 2015), to post-12 Ma orogenlarge-scale 'horizontal tectonics, accompanied by orogen perpendicular growth of the Alps,tectonics' cannot be explained by a classical model of continent-continent collision and continuous foreland propagation of the orogenic wedge. In the following, we discuss the observed exhumation pattern along the Subalpine Molasse (Fig. 6a) in the context of the post-35 Ma tectonic evolution of the Central Alpine orogeny as proposed by Kissling and Schlunegger (2018) and Schlunegger and Kissling (2015)), and we argue for a deep-driver to controlcontrolling the large-wavelength thrusting in the North Alpine foreland and the proposed transition from dominantly verticalbuoyancy-driven 'vertical' to 'horizontal tectonics, associated with widespread tectonic activity in the foreland and a period of orogenic wideningtectonics' thereafter.

During the Alpine orogeny, convergence rates between the Adriatic and European continental plates decreased when the positively buoyant European continental crust started to enter the subduction zone ca. 35 My ago (Fig. 8b; Handy et al., 2010; Schmid et al., 1996) and when ~~delamination and~~ wedging of European continental crust was initiated (Schmid et al., 1996). Large slab pull forces exerted by the negatively buoyant oceanic lithospheric slab induced extensional forces within the subducting plate, which led to necking and possibly eventually to slab breakoff (Davies and von Blanckenburg, 1995). ~~Subsequent slab unloading caused strong uplift and backthrusting along the Insubric Line (Berger et al., 2011; Hurford, 1986; Schmid et al., 1996).~~ According to Kissling (2008) and Kissling and Schlunegger (2018), the ~~delaminated and thus~~ dense European mantle slab, which was still attached to the foreland plate but delaminated (i.e. separated) from the crust, continued to roll back, with the consequence ~~of~~that the slab ~~steepening~~steepened and ~~northward migration of~~that the locus of crustal delamination migrated northward. ~~T~~his forced new crustal material to enter the subduction system and to become stacked to the Alpine edifice ~~as evidenced by~~in the ~~emplacement~~form of ~~the~~crystalline and sedimentary nappes (e.g. Helvetic nappes (Fig. 8c), or alternatively it was accreted to the crustal root through the basal accretion of mid-crustal material (Fry et al., 2010). Ongoing ~~slab~~ roll-back subduction and an associated increase in the lower ~~plate~~plate's flexure ~~resulted~~is probably reflected in ~~a~~the northward propagation of the northern margin of the Central Alps' Molasse Basin until ca. 20-18 Ma (Fig. 8

Thereafter, plate convergence rates seemed to decrease noticeably (Fig. 8b; Handy et al., 2010; Schmid et al., 1996). At this stage, pro-wedge widening of the Molasse Basin came to a relative halt~~.~~ (Fig. 8a). In the Central Alps, the proximal part of the basin kept subsiding by additional 2-3 km (~~Fig. 8a;~~Burkhard and Sommaruga, 1998; Schlunegger and Kissling, 2015), while the distal realm became subject to erosion (Kuhlemann and Kempf, 2002). This phase was also associated with the period of buoyancy-driven differential vertical ~~tectonics~~uplift of the ~~ECMs,~~Aar Massif (and probably also the Mont Blanc and Aiguilles Rouges Massifs), i.e. ~~their~~its rise along steeply dipping reverse shear zones between ca. 20 Ma and 12 Ma (Herwegh et al., 2017, 2020; Wehrens et al., 2017), while the northern deformation front remained stationary in the Subalpine Molasse (Fig. 8c; Burkhard and Sommaruga, 1998; von Hagke et al., 2014b; Ortner et al., 2015). East of Munich, however, the Molasse Basin experienced, at this time, a period of uniform subsidence and even a short-lived phase of uplift (ca. 17-16 Ma) as evidenced by horizontal to 5° westward tilting strata of post-20 My old Molasse sediments (Gusterhuber et al., 2012; Zweigel et al., 1998). ~~This~~The latter was attributed to ~~a decrease in surface loads in the orogen in response to~~eastward-directed lateral extrusion ~~(i.e. escape tectonics) and a corresponding lowering of the Eastern Alps' topography~~of crustal blocks (Gusterhuber et al., 2012~~;~~). It also correlates with the observed westward increasing gradient of crustal thickening associated with an eastward decrease of the Eastern Alps' average elevation (Rosenberg et al., 2018). Alternatively, Handy et al. (2015) explained this signal as a result of deep crustal unloading due to a proposed slab tear and a corresponding subduction polarity reversal beneath the Eastern Alps. These observations imply that important along-strike changes and a large-scale geodynamic (Hetényi et al., 2018b; Kissling et al., 2006; Lippitsch et al., 2003; Mitterbauer et al., 2011) and tectonic (e.g. Handy et al., 2015;

Ratschbacher et al., 1991; Rosenberg et al., 2018) decoupling between the Central and the Eastern Alps and their Molasse Basins have been established by the end of mid-Miocene times.

This is also mirrored by the along-strike changespattern in the late Miocene cumulative horizontal shortening in the North Alpine foreland, which decreases, without fully considering the possibly large uncertainties of shortening estimation in the Subalpine Molasse, seems to decrease from >30 km near Lake Geneva, to ca. 20 km near Lake Constance, and finally . A rapid decrease from ca. 18 km to <1 km near over a lateral distance of just ca. 120 km is finally recorded between ca. 10.5° E and Salzburg (Fig. 6). East of Salzburg at the front of the Eastern Alps, zero late Miocene shortening is recorded in the proximal Molasse. (Beidinger and Decker, 2014; Hinsch, 2013; Ortner et al., 2015). This pattern has been attributed to an increasing transfer of shortening towards the internal parts of the orogen (i.e. the Tauern Window) and to the out-of-section removal of crust through lateral extrusion in the Eastern Alps (Ortner et al., 2006, 2015). While such upper crustal processes may certainly mask the signal of late Miocene foreland deformation, the latter may also reflect the response to the change of a geodynamic driving force operating at a larger scale, situated at deeper crustal levels, and encompassing the entire Central Alps until as far east as 12.8° E (near Salzburg; Fig. 9). The attached European lithospheric slab beneath the Central Alps presents here a possible candidate for driving the observed large wavelength signal of late Miocene foreland deformation (Fig. 9). This hypothesis is based on the following main observations and considerations: (i) The along-strike extent of late Miocene thrusting in the foreland correlates spatially remarkably well with the proposed extent of the steeply south-dipping Central Alpine European slab imaged by seismic tomography (Fig. 9).9; Kästle et al., 2020; Lippitsch et al., 2003; Zhao et al., 2016). (ii) The large spatial wavelength of tectonically driven exhumation of the tectonic signal, which at least in the Subalpine Molasse, which has been attributed to distinct thrusting events between Lake Thun and Lake Constance seems to occur in the form of individual tectonic pulses, likely excludes more localca. 12-4 Ma, can be viewed as an upper crustal phenomena as possible drivers and points towards bigger players such as plate tectonics or slab dynamics.expression of a lithospheric-scale tectonic driver acting at that wavelength. (iii) The proposed segmentation of the deep structure of the Central and Eastern Alps (i.e. slab detachment and subduction polarity reversal; Handy et al., 2015; Hetényi et al., 2018b; Kästle et al., 20192020; Kissling et al., 2006; Lippitsch et al., 2003; Mitterbauer et al., 2011; Schmid et al., 2004), which is expected to have induced a geodynamic and tectonic reorganization along the Alpine chain by the end of mid-Miocene times could explain the subsequent late Miocene tectonism, which was restricted to the foreland of the Central Alps until ca. Salzburg and which was thus decoupled from the Eastern Alps. The corresponding changetransition in the macro-tectonic regime of the northern Central Alps from dominantly verticalbuoyancy-driven 'vertical' to large-scale 'horizontal tectonicstectonics' may reflect decreasing rates of European slab rollback and a late phase of post-collisional indentation of Adria as recently proposed by Herwegh et al. (2017) and Kissling and Schlunegger (2018; 2020).

5.2.3 The exceptional position of the Bavarian Subalpine Molasse

The configuration of the lithospheric mantle slabs is inherently different beneath the Central and the Eastern Alps (Kästle et al., 2020; Kissling et al., 2006; Kissling and Schlunegger, 2018; Lippitsch et al., 2003; Mitterbauer et al., 2011; Zhao et al., 2016). At the lithospheric scale, a polarity reversal between the European slab and the Adriatic slab has been conjectured

5   beneath the western Tauern Window (Lippitsch et al., 2003). However, this model is currently debated as new geophysical data indicate that at depth the southward dipping European slab extends from the Central Alps until east of the Giudicarie and Brenner Faults (Kästle et al., 20192020) and possibly as far east as 12.5° E, i.e. the central Tauern Window (Figs. 1 and 9; Qorbani et al., 2015). Although theBased on tomographic results from the AlpArray intiative, Hetényi et al. (2018b) propose that at ca. 13° E a northward-dipping slab of the Adriatic plate is present. All these studies show that the deep structure remains

10   very uncertain and debated since tomographic data have been interpreted in different ways regarding the slab geometries at depth (Hetényi et al., 2018b; Kästle et al., 20192020; Lippitsch et al., 2003; Mitterbauer et al., 2011; Zhao et al., 2016), most of them). However, they all concur on the observation that between the deep velocity anomalies of the Central and the Eastern Alps a major discontinuity is present east of the Giudicarie and Brenner Faults (see also Handy et al., 2015). This correlates with the eastward termination of the late Miocene Subalpine Molasse near Salzburg (Fig. 9). Hence, the geophysical data place

15   the link between the deep structure and deformation of the Subalpine Molasse between Lake Constance and Salzburg in a Central Alpine rather than an Eastern Alpine context.

While at the mantle scale, a segmentation of the slab structure is observed at ca. 12.5° E (Fig. 9), an along-strike segmentation at crustal levels occurs further west (at the Brenner Fault). East of the Brenner Fault (Figs. 1 and 9), the post-collisional evolution of the Eastern Alps is characterized by the northward indentation of the Dolomite indenter and the related eastward

20   lateral extrusion of crustal blocks (Ratschbacher et al., 1991). At the larger scale, this was possibly facilitated by slab retreat beneath the Carpathians and the associated rifting in the Pannonian Basin (Peresson and Decker, 1997). The main phase of lateral extrusion occurred in early and mid-Miocene times (Frisch et al., 1998; Ratschbacher et al., 1991), possibly extending into the late Miocene (Ortner et al., 2015). These processes were additionally associated with the collisional exhumation of the Tauern Window and normal faulting along its bounding low-angle normal faults (see Rosenberg et al., 2018). In this respect,

25   the Bavarian Subalpine Molasse is particularly interesting, since it extends over this transition area (Fig. 9). In this transient position, the tectonics of this segment of the Subalpine Molasse between Lake Constance and Salzburg was probably affected by the deep-seated dynamics of the Central Alpine European slab, while at the same time tectonic processes related to slab dynamics were possiblybeing also masked by the aforementioned upper crustal processes of Eastern Alpine tectonics (e.g. lateral extrusion).

30   For resolving the influence of deep-seated processes on the tectonics of the Subalpine Molasse and the foreland basin in general, the present-day slab geometries underneath the entire Alps must be resolved at higher resolution. Furthermore, the time-evolution of the slabs must be constrained with a focus on if, when, and how a potential subduction polarity reversal

occurred in the Eastern Alps. These studies should be supported by source-to-sink analyses linking the stratigraphy of the foreland to hinterland processes. New thermochronological data from the Bavarian Subalpine and Foreland (i.e. undeformed) Molasse will be essential. Furthermore, we expect that ongoing seismo-tomographic investigations will disclose further details to constrain the deep-seated driving mechanisms (Hetényi et al., ~~2018~~2018a).

6 Conclusions

In this paper, we presented new low-temperature thermochronological age data from the Subalpine Molasse of the Central European Alps. By comparing our results to published age and stratigraphic data along-strike the Alps from Lake Geneva to Salzburg we conclude that:

- (U-Th-Sm)/He ages along the Subalpine Molasse of the Central Alps ~~are consistently~~record thrust-related exhumation between 12-4 Ma ~~and can be assigned to~~with at least two ~~tectonic pulses~~thrusting event associated with it at ca. 10 and 6 Ma.

- The pattern of strain ~~release~~accommodation is strongly conditioned by the local-scale mechanical stratigraphy, since the locus of deformation depends on the distribution of mechanically weak (sand- and mudstones) and strong (conglomerates) lithologies. Accordingly, a general widening of the foreland thrust-belt (i.e. tectonic salients) and en-bloc deformation of large conglomerate bodies occurs at the locations where the stratigraphy is conglomerate dominated, i.e. at the site of former megafan dispersal systems depositing large and km-thick conglomerate sequences into the foreland. Conversely, tectonic recesses and a more distributed deformation pattern developed where the mechanical stratigraphy is dominated by sand- and mudstone deposits.

- ~~Despite the~~The along-strike highly non-cylindrical hinterland ~~exhumation history and~~architecture, and the variability of the sites of exhumation of the former basement of the European margin has no apparent imprint on the distribution of late Miocene ~~tectonic signal~~shortening recorded in the Subalpine Molasse ~~is remarkably constant along-strike the Alps, from Lake Geneva to Salzburg~~and the Jura fold-and-thrust belt.

Hence, we observe that the deformation style during late Miocene thrusting of the Subalpine Molasse is masked by local variations in the stratigraphic architecture. However, ~~the overall tectonic signal~~in terms of timing and kinematics, thrust-related shortening, though decreasing in intensity from the west to the east, is consistent ~~in terms of timing and kinematics~~along-strike ~~the part~~in those parts of the Alps which ~~correlates~~correlate with the lateral (i.e. along-strike) extent of the Central Alpine lithospheric mantle slab at depth. ~~Large-wavelength~~Thus, we may interpret late Miocene large-wavelength thrusting ~~may thus be interpreted~~ as an upper crustal signal resulting from changes of this lithospheric driving force. The latter possibly leads to a ~~prominent~~change in the macro-tectonic regime in this sector of the Alpine orogen at ca. 12 Ma, from ~~dominantly vertical~~buoyancy-driven 'vertical' to ~~horizontal~~thrusting-dominated 'horizontal' tectonics.

54

In summary, although we lack the required data to precisely determine the geodynamic processes responsible for the late phase of shortening in the Molasse, we are able to constrain the timing of this event to 12-4 Ma. In addition, this work shows that low-temperature thermochronological data yield an improved understanding of the chronology of orogenic processes where the late orogenic stage of a mountain belt may be characterized by a complex pattern of strain release conditioned by site-specific stratigraphic and thus lithological conditions at the local scale, and by ~~a change from vertical to horizontal tectonics at the larger scale including the entire Central Alps~~widespread tectonism possibly resulting from changes in deep seated driving forces.

Appendix A: Apatite separation and picking

~~To release the apatite crystals from the rock samples, we used the electrodynamic disaggregation technique (selFrag). This method exposes the rock specimen to a high voltage pulse and fractures it along its grain boundaries. As opposed to separation using a jaw crusher, this method is less time consuming and the rock is disintegrated along the grain boundaries (Giese et al., 2010). This ensures individual grains are less prone to damaging during processing.~~

~~To prepare the samples for electrodynamic disaggregation, they had to be crushed into fist-sized pieces by hand using a hammer. This was necessary due to the limiting dimensions of the processing vessel of the selFrag. For releasing the individual grains, we applied a frequency of 3 Hz and electric potentials of 130-150 kV, depending on the hardness of the rock. For every sample, the electrode distance was incrementally reduced in 5 mm steps from a maximum of 40 mm to a minimum of 15 mm. Per step, a minimum of 20 pulses was applied to ensure full release of the individual grains. It has been shown that the influence of diffusive loss of ^{4}He due to the plasma channel hitting the apatite crystal is negligible, and (U-Th-Sm)/He (AHe) ages from samples separated with electrodynamic disaggregation are indistinguishable from AHe ages measured on apatites released with mechanical techniques (Giese et al., 2010).~~

~~Apatite crystals were concentrated using standard rock separation techniques. First, the grain size fraction of 64-250 μm, which is suitable for AHe dating, was separated using disposable sieving meshes. To remove magnetic minerals from the sieved sample fraction, we used a Frantz magnetic separator at 0.5 A and 1.2 A. To concentrate apatite from the remaining grains, we used lithium based tungstate (ρ = 2.81 g cm^{-3}) as heavy liquid for density separation of the heavy minerals. On average, we had to process ca. 100 g of sample material to acquire enough heavy minerals. The heavy mineral fraction has been thoroughly rinsed with deionized water and then dried at 30°C.~~

~~Apatites have been hand-picked under a binocular and checked for inclusions and imperfections under an optical microscope with cross-polarized light. Wherever possible, we selected euhedral, intact, and inclusion free grains with a minimum width of 60 μm. However, as the grains are detrital, partly grains with rough surfaces or tiny fluid inclusions had to be picked. This may result in larger error bars or even grain ages that do not yield a geologically meaningful age. These ages were excluded (see section 3.2 and Table 1).~~

Data availability

The research data is enclosed in this paper and can be freely accessed.

Author contribution

SM designed the study with support from MH, FS, and CvH. FS and MH assisted SM during sampling in the field. SM carried out mineral separation and picked the apatite crystals. ID carried out the helium extraction and the ICP-MS measurements at University of Göttingen. CvH and ID assisted in analyzing and interpreting the apatite (U-Th-Sm)/He ages. SM prepared the manuscript, with contributions from all co-authors.

Competing interests

The authors declare that they have no conflict of interest.

Acknowledgements

We thank Judith Dunkl (Göttingen) for assisting in the selection of apatite crystals, Pierre Valla (Bern) for discussions on the AHe ages and the thermal models, and Edi Kissling (Zurich) for his insights on lithospheric scale processes. The manuscript has greatly benefited by detailed and constructive comments by Claudio Rosenberg (Paris), Giovanni Luca Cardello (Rome) Hugo Ortner (Innsbruck) and Nicola Levi (Vienna). Additional information of the data can be found in the supplementary material. The study was funded by the Swiss Geological Survey of the Federal Office of Topography (swisstopo) as part of the GeoMol CH project. We acknowledge the use of the Move Software Suite (used for Fig. 5) granted by ~~Midland Valley's Academic Software Initiative~~Petroleum Experts Limited.

References

Allen, P. A., Crampton, S. L. and Sinclair, H. D.: The inception and early evolution of the North Alpine Foreland Basin, Switzerland, Basin Res., 3(3), 143–163, doi:10.1111/j.1365-2117.1991.tb00124.x, 1991.

Aubert, D.: Sur l'existence d'une ride de plissement oligocène dans le Jura vaudois, Bull. la Société Neuchâteloise des Sci. Nat., 81, 47–54, 1958.

Bachmann, G. H. and Müller, M.: Sedimentary and structural evolution of the German Molasse Basin, Eclogae Geol. Helv., 85(3), 519–530, doi:10.5169/seals-167019, 1992.

Baran, R., Friedrich, A. M. and Schlunegger, F.: The late Miocene to Holocene erosion pattern of the Alpine foreland basin

reflects Eurasian slab unloading beneath the western Alps rather than global climate change, Lithosphere, 6(2), 124–131, doi:10.1130/L307.1, 2014.

Beck, P.: Über den Mechanismus der subalpinen Molassetektonik, Eclogae Geol. Helv., 38(2), 353–368, 1945.

Becker, A.: The Jura Mountains — an active foreland fold-and-thrust belt?, Tectonophysics, 321(4), 381–406, doi:10.1016/S0040-1951(00)00089-5, 2000.

Beidinger, A. and Decker, K.: Quantifying Early Miocene in-sequence and out-of-sequence thrusting at the Alpine-Carpathian junction, Tectonics, 33(3), 222–252, doi:10.1002/2012TC003250, 2014.

Bellahsen, N., Mouthereau, F., Boutoux, A., Bellanger, M., Lacombe, O., Jolivet, L. and Rolland, Y.: Collision kinematics in the western external Alps, Tectonics, 33(6), 1055–1088, doi:10.1002/2013TC003453, 2014.

Berge, T. B. and Veal, S. L.: Structure of the Alpine foreland, Tectonics, 24(5), TC5011, doi:10.1029/2003TC001588, 2005.Berger, A., Schmid, S. M., Engi, M., Bousquet, R. and Wiederkehr, M.: Mechanisms of mass and heat transport during Barrovian metamorphism: A discussion based on field evidence from the Central Alps (Switzerland/northern Italy), Tectonics, 30(1), TC1007, doi:10.1029/2009TC002622, 2011.

Berger, A., Wehrens, P., Lanari, P., Zwingmann, H. and Herwegh, M.: Microstructures, mineral chemistry and geochronology of white micas along a retrograde evolution: An example from the Aar massif (Central Alps, Switzerland), Tectonophysics, 721(March), 179–195, doi:10.1016/j.tecto.2017.09.019, 2017.

Blau, R. V.: Molasse und Flysch im östlichen Gurnigelgebiet (Kt. Bern), Beiträge zur Geol. Karte der Schweiz, NF 125, 151 pp., 1966.

Boston, K. R., Rubatto, D., Hermann, J., Engi, M. and Amelin, Y.: Geochronology of accessory allanite and monazite in the Barrovian metamorphic sequence of the Central Alps, Switzerland, Lithos, 286–287, 502–518, doi:10.1016/j.lithos.2017.06.025, 2017.

Boutoux, A., Bellahsen, N., Nanni, U., Pik, R., Verlaguet, A., Rolland, Y. and Lacombe, O.: Thermal and structural evolution of the external Western Alps: Insights from (U–Th–Sm)/He thermochronology and RSCM thermometry in the Aiguilles Rouges/Mont Blanc massifs, Tectonophysics, 683, 109–123, doi:10.1016/j.tecto.2016.06.010, 2016.

Boyer, S. E. and Elliott, D.: Thrust systems, Am. Assoc. Pet. Geol. Bull., 66(9), 1196–1230, 1982.

Burkhard, M.: Aspects of the large-scale Miocene deformation in the most external part of the Swiss Alps (Subalpine Molasse to Jura fold belt), Eclogae Geol. Helv., 83(3), 559–583, 1990.

Burkhard, M. and Sommaruga, A.: Evolution of the western Swiss Molasse basin: structural relations with the Alps and the Jura belt, Geol. Soc. London, Spec. Publ., 134(1), 279–298, doi:10.1144/GSL.SP.1998.134.01.13, 1998.

Buxtorf, A.: Prognosen und Befunde beim Hauensteinbasis- und Grenchenbergtunnel und die Bedeutung der letzteren für die Geologie des Juragebirges, Verhandlungen der Naturforschenden Gesesellschaft Basel, 27, 184–254, 1916.

Caputo, R., Poli, M. E. and Zanferrari, A.: Neogene–Quaternary tectonic stratigraphy of the eastern Southern Alps, NE Italy, J. Struct. Geol., 32(7), 1009–1027, doi:10.1016/j.jsg.2010.06.004, 2010.

5 Cardello, G. L., Di Vincenzo, G., Giorgetti, G., Zwingmann, H. and Mancktelow, N.: Initiation and development of the Pennine Basal Thrust (Swiss Alps): a structural and geochronological study of an exhumed megathrust, J. Struct. Geol., 126, 338–356, doi:10.1016/j.jsg.2019.06.014, 2019.

Castellarin, A. and Cantelli, L.: Neo-Alpine evolution of the Southern Eastern Alps, J. Geodyn., 30(1–2), 251–274, doi:10.1016/S0264-3707(99)00036-8, 2000.

10 Cederbom, C. E., Sinclair, H. D., Schlunegger, F. and Rahn, M. K.: Climate-induced rebound and exhumation of the European Alps, Geology, 32(8), 709, doi:10.1130/g20491.1, 2004.

Cederbom, C. E., van der Beek, P., Schlunegger, F., Sinclair, H. D. and Oncken, O.: Rapid extensive erosion of the North Alpine foreland basin at 5-4 Ma, Basin Res., 23(5), 528–550, doi:10.1111/j.1365-2117.2011.00501.x, 2011.

Champagnac, J.-D., Molnar, P., Anderson, R. S., Sue, C. and Delacou, B.: Quaternary erosion-induced isostatic rebound in the 15 western Alps, Geology, 35(3), 195, doi:10.1130/G23053A.1, 2007.

Chemenda, A. I., Burg, J. P. and Mattauer, M.: Evolutionary model of the Himalaya-Tibet system: Geopoem based on new modelling, geological and geophysical data, Earth Planet. Sci. Lett., 174(3–4), 397–409, doi:10.1016/S0012-821X(99)00277-0, 2000.

Davies, J. H. and von Blanckenburg, F.: Slab breakoff: A model of lithosphere detachment and its test in the magmatism and 20 deformation of collisional orogens, Earth Planet. Sci. Lett., 129(1–4), 85–102, doi:10.1016/0012-821X(94)00237-S, 1995.

DeCelles, P. G. and Giles, K. A.: Foreland basin systems, Basin Res., 8(2), 105–123, doi:10.1046/j.1365-2117.1996.01491.x, 1996.

Dürst Stucki, M., Reber, R. and Schlunegger, F.: Subglacial tunnel valleys in the Alpine foreland: an example from Bern, Switzerland, Swiss J. Geosci., 103(3), 363–374, doi:10.1007/s00015-010-0042-0, 2010.

25 Egli, D., Mosar, J., Ibele, T. and Madritsch, H.: The role of precursory structures on Tertiary deformation in the Black Forest— Hegau region, Int. J. Earth Sci., doi:10.1007/s00531-016-1427-8, 2016.

Egli, D., Mancktelow, N. and Spikings, R.: Constraints from 40 Ar/ 39 Ar geochronology on the timing of Alpine shear zones in the Mont Blanc-Aiguilles Rouges region of the European Alps, Tectonics, 36(4), 730–748, doi:10.1002/2016TC004450, 2017.

Farley, K. A.: (U-Th)/He Dating: Techniques, Calibrations, and Applications, Rev. Mineral. Geochemistry, 47(1), 819–844, doi:10.2138/rmg.2002.47.18, 2002.

Farley, K. A., Wolf, R. A. and Silver, L. T.: The effects of long alpha-stopping distances on (U-Th)/He ages, Geochim. Cosmochim. Acta, 60(21), 4223–4229, doi:10.1016/S0016-7037(96)00193-7, 1996.

5   Fillon, C., Huismans, R. S. and van der Beek, P.: Syntectonic sedimentation effects on the growth of fold-and-thrust belts, Geology, 41(1), 83–86, doi:10.1130/G33531.1, 2013.

Fox, M., Herman, F., Willett, S. D. and Schmid, S. M.: The Exhumation history of the European Alps inferred from linear inversion of thermochronometric data, Am. J. Sci., 316(6), 505–541, doi:10.2475/06.2016.01, 2016.

Frisch, W., Kuhlemann, J., Dunkl, I. and Brügel, A.: Palinspastic reconstruction and topographic evolution of the Eastern Alps
10   during late Tertiary tectonic extrusion, Tectonophysics, 297(1–4), 1–15, doi:10.1016/S0040-1951(98)00160-7, 1998.

Fry, B., Deschamps, F., Kissling, E., Stehly, L. and Giardini, D.: Layered azimuthal anisotropy of Rayleigh wave phase velocities in the European Alpine lithosphere inferred from ambient noise, Earth Planet. Sci. Lett., 297(1–2), 95–102, doi:10.1016/j.epsl.2010.06.008, 2010.

Fuchs, W.: Gedanken zur Tektogenese der nördlichen Molasse zwischen Rhone und March, Jahrb. der Geol. Bundesanstalt,
15   119(2), 207–249, 1976.

Ganss, O. and Schmidt-Thomé, P.: Die gefaltete Molasse am Alpenrand zwischen Bodensee und Salzach, Zeitschrift der Dtsch. Geol. Gesellschaft, 105, 402–495, 1953.

Ganti, V., von Hagke, C., Scherler, D., Lamb, M. P., Fischer, W. W. and Avouac, J.-P.: Time scale bias in erosion rates of glaciated landscapes, Sci. Adv., 2(10), e1600204, doi:10.1126/sciadv.1600204, 2016.

20   Garefalakis, P. and Schlunegger, F.: Link between concentrations of sediment flux and deep crustal processes beneath the European Alps, Sci. Rep., 8(1), 183, doi:10.1038/s41598-017-17182-8, 2018.

Genser, J., Cloetingh, S. and Neubauer, F.: Late orogenic rebound and oblique Alpine convergence: New constraints from subsidence analysis of the Austrian Molasse basin, Glob. Planet. Change, 58(1–4), 214–223, doi:10.1016/j.gloplacha.2007.03.010, 2007.

25   Giamboni, M., Ustaszewski, K., Schmid, S. M., Schumacher, M. E. and Wetzel, A.: Plio-Pleistocene transpressional reactivation of Paleozoic and Paleogene structures in the Rhine-Bresse transform zone (northern Switzerland and eastern France), Int. J. Earth Sci., 93(2), 207–223, doi:10.1007/s00531-003-0375-2, 2004.

Giese, J., Seward, D., Stuart, F. M., Wüthrich, E., Gnos, E., Kurz, D., Eggenberger, U. and Schreurs, G.: Electrodynamic Disaggregation: Does it Affect Apatite Fission-Track and (U-Th)/He Analyses?, Geostand. Geoanalytical Res., 34(1), 39–48,

doi:10.1111/j.1751-908X.2009.00013.x, 2010.

Glotzbach, C., Reinecker, J., Danišík, M., Rahn, M. K., Frisch, W. and Spiegel, C.: Thermal history of the central Gotthard and Aar massifs, European Alps: Evidence for steady state, long-term exhumation, J. Geophys. Res., 115, F03017, doi:10.1029/2009JF001304, 2010.

5   Guellec, S., Mugnier, J.-L., Tardy, M. and Roure, F.: Neogene evolution of the western Alpine foreland in the light of ECORS data and balanced cross-section, in Deep structure of the Alps, Mém. Soc. géol. suisse, vol. 1, edited by F. Roure, P. Heitzmann, and R. Polino, pp. 165–184, Société Geologique Suisse, Zürich., 1990.

Gusterhuber, J., Dunkl, I., Hinsch, R., Linzer, H.-G. and Sachsenhofer, R.: Neogene uplift and erosion in the Alpine Foreland Basin (Upper Austria and Salzburg), Geol. Carpathica, 63(4), 295–305, doi:10.2478/v10096-012-0023-5, 2012.

10   von Hagke, C. and Malz, A.: Triangle zones – Geometry, kinematics, mechanics, and the need for appreciation of uncertainties, Earth-Science Rev., 177(November 2017), 24–42, doi:10.1016/j.earscirev.2017.11.003, 2018.

von Hagke, C., Cederbom, C. E., Oncken, O., Stöckli, D. F., Rahn, M. K. and Schlunegger, F.: Linking the northern Alps with their foreland: The latest exhumation history resolved by low-temperature thermochronology, Tectonics, 31(5), TC5010, doi:10.1029/2011TC003078, 2012.

15   von Hagke, C., Oncken, O. and Evseev, S.: Critical taper analysis reveals lithological control of variations in detachment strength: An analysis of the Alpine basal detachment (Swiss Alps), Geochemistry, Geophys. Geosystems, 15(1), 176–191, doi:10.1002/2013GC005018, 2014a.

von Hagke, C., Oncken, O., Ortner, H., Cederbom, C. E. and Aichholzer, S.: Late Miocene to present deformation and erosion of the Central Alps — Evidence for steady state mountain building from thermokinematic data, Tectonophysics, 632, 250–
20   260, doi:10.1016/j.tecto.2014.06.021, 2014b.

Haldemann, E. G., Haus, H. A., Holliger, A., Liechti, W., Rutsch, R. F. and della Valle, G.: Geological Atlas of Switzerland 1:25000, Map sheet Eggiwil (LK 1188), Federal Office of Topography swisstopo, Wabern, Switzerland., 1980.

Handy, M. R., Schmid, S. M., Bousquet, R., Kissling, E. and Bernoulli, D.: Reconciling plate-tectonic reconstructions of Alpine Tethys with the geological–geophysical record of spreading and subduction in the Alps, Earth-Science Rev., 102(3–4),
25   121–158, doi:10.1016/j.earscirev.2010.06.002, 2010.

Handy, M. R., Ustaszewski, K. and Kissling, E.: Reconstructing the Alps–Carpathians–Dinarides as a key to understanding switches in subduction polarity, slab gaps and surface motion, Int. J. Earth Sci., 104(1), 1–26, doi:10.1007/s00531-014-1060-3, 2015.

Haus, H.: Über alte Erosionserscheinungen am Südrand der miocaenen Nagelfluh des oberen Emmentales und deren
30   Bedeutung für die Tektonik des Alpenrandes, Eclogae Geol. Helv., 28(2), 667–677, 1935.

Haus, H.: Geologie der Gegend von Schangnau im oberen Emmental (Kanton Bern): ein Beitrag zur Stratigraphie und Tektonik der subalpinen Molasse und des Alpenrandes, Beiträge zur Geol. Karte der Schweiz, NF 75, 106 pp., 1937.

Herwegh, M., Berger, A., Baumberger, R., Wehrens, P. and Kissling, E.: Large-Scale Crustal-Block-Extrusion During Late Alpine Collision, Sci. Rep., 7, 413, doi:10.1038/s41598-017-00440-0, 2017.

5   Herwegh, M., Berger, A., Glotzbach, C., Wangenheim, C., Mock, S., Wehrens, P., Baumberger, R., Egli, D. and Kissling, E.: Late ~~Stages~~stages of ~~Continent Continent Collision~~continent-continent collision: Timing, ~~Kinematic Evolution~~kinematic evolution, and ~~Exhumation~~exhumation of the Northern ~~Rim~~rim (Aar Massif) of the Alps, Earth Sci. Rev., ~~n.d~~200, 102959, doi:10.1016/j.earscirev.2019.102959, 2020.

Hetényi, G., Molinari, I., Clinton, J., Bokelmann, G., Bondár, I., Crawford, W. C., Dessa, J.-X., Doubre, C., Friederich, W.,
10   Fuchs, F., Giardini, D., Gráczer, Z., Handy, M. R., Herak, M., Jia, Y., Kissling, E., Kopp, H., Korn, M., Margheriti, L., Meier, T., Mucciarelli, M., Paul, A., Pesaresi, D., Piromallo, C., Plenefisch, T., Plomerová, J., Ritter, J., Rümpker, G., Šipka, V., Spallarossa, D., Thomas, C., Tilmann, F., Wassermann, J., Weber, M., Wéber, Z., Wesztergom, V. and Živčić, M.: The AlpArray Seismic Network: A Large-Scale European Experiment to Image the Alpine Orogen, Surv. Geophys., 39(5), 1009–1033, doi:10.1007/s10712-018-9472-4, ~~2018~~2018a.

15   Hetényi, G., Plomerová, J., Bianchi, I., Kampfová Exnerová, H., Bokelmann, G., Handy, M. R. and Babuška, V.: From mountain summits to roots: Crustal structure of the Eastern Alps and Bohemian Massif along longitude 13.3°E, Tectonophysics, 744, 239–255, doi:10.1016/j.tecto.2018.07.001, 2018b.

Hinsch, R.: Laterally varying structure and kinematics of the Molasse fold and thrust belt of the Central Eastern Alps: Implications for exploration, Am. Assoc. Pet. Geol. Bull., 97(10), 1805–1831, doi:1 0.1306/04081312129, 2013.

20   Homewood, P., Allen, P. A. and Williams, G. D.: Dynamics of the Molasse Basin of Western Switzerland, in Foreland Basins, pp. 199–217, Blackwell Publishing Ltd., Oxford, UK., 1986.

Hourigan, J. K., Reiners, P. W. and Brandon, M. T.: U-Th zonation-dependent alpha-ejection in (U-Th)/He chronometry, Geochim. Cosmochim. Acta, 69(13), 3349–3365, doi:10.1016/j.gca.2005.01.024, 2005.

Hurford, A. J.: Cooling and uplift patterns in the Lepontine Alps South Central Switzerland and an age of vertical movement
25   on the Insubric fault line, Contrib. to Mineral. Petrol., 92(4), 413–427, doi:10.1007/BF00374424, 1986.

Ji, W., Malusà, M. G., Tiepolo, M., Langone, A., Zhao, L. and Wu, F.: Synchronous Periadriatic magmatism in the Western and Central Alps in the absence of slab breakoff, Terra Nov., 31(2), 120–128, doi:10.1111/ter.12377, 2019.

Jordi, H. A.: Blatt 1188 Eggiwil, Geol. Atlas Schweiz 1 25 000, Erläut. 75, 2012.

Karner, G. D. and Watts, A. B.: Gravity anomalies and flexure of the lithosphere at mountain ranges, J. Geophys. Res. Solid
30   Earth, 88(B12), 10449–10477, doi:10.1029/JB088iB12p10449, 1983.

Kästle, E. D., Rosenberg, C., Boschi, L., Bellahsen, N., Meier, T. and El-Sharkawy, A.: Slab ~~Break~~break-offs in the Alpine ~~Subduction Zone, Solid~~subduction zone, Int. J. Earth ~~Discuss., (January), 1–16~~Sci., 109(2), 587–603, doi:10.~~5194/se-2019-17, 2019~~1007/s00531-020-01821-z, 2020.

Kempf, O., Matter, A., Burbank, D. W. and Mange, M.: Depositional and structural evolution of a foreland basin margin in a magnetostratigraphic framework: the eastern Swiss Molasse Basin, Int. J. Earth Sci., 88(2), 253–275, doi:10.1007/s005310050263, 1999.

Ketcham, R. A.: Forward and Inverse Modeling of Low-Temperature Thermochronometry Data, Rev. Mineral. Geochemistry, 58(1), 275–314, doi:10.2138/rmg.2005.58.11, 2005.

Kissling, E.: Deep structure and tectonics of the Valais - And the rest of the Alps, Bull. fuer Angew. Geol., 13(2), 3–10, 2008.

Kissling, E. and Schlunegger, F.: Rollback Orogeny Model for the Evolution of the Swiss Alps, Tectonics, 37(4), 1097–1115, doi:10.1002/2017TC004762, 2018.

Kissling, E., Schmid, S. M., Lippitsch, R., Ansorge, J. and Fügenschuh, B.: Lithosphere structure and tectonic evolution of the Alpine arc: new evidence from high-resolution teleseismic tomography, Geol. Soc. London, Mem., 32(1), 129–145, doi:10.1144/GSL.MEM.2006.032.01.08, 2006.

Kuhlemann, J. and Kempf, O.: Post-Eocene evolution of the North Alpine Foreland Basin and its response to Alpine tectonics, Sediment. Geol., 152(1–2), 45–78, doi:10.1016/S0037-0738(01)00285-8, 2002.

Lacombe, O. and Mouthereau, F.: Basement-involved shortening and deep detachment tectonics in forelands of orogens: Insights from recent collision belts (Taiwan, Western Alps, Pyrenees), Tectonics, 21(4), 1030, doi:10.1029/2001TC901018, 2002.

Landesgeologie: Geological Map of Switzerland 1:500'000, Federal Office of Topography swisstopo, Wabern, Switzerland., 2005.

Landesgeologie: GeoMol: Geologisches 3D-Modell des Schweizer Molassebeckens - Schlussbericht, Berichte der Landesgeologie, 10, 128 pp., 2017.

Laubscher, H. P.: Die Fernschubhypothese der Jurafaltung, Eclogae Geol. Helv., 54(1), 221–280, 1961.

Laubscher, H. P.: Jura kinematics and the Molasse Basin, Eclogae Geol. Helv., 85(3), 653–675, 1992.

Leary, R., Orme, D. A., Laskowski, A. K., DeCelles, P. G., Kapp, P., Carrapa, B. and Dettinger, M.: Along-strike diachroneity in deposition of the Kailas Formation in central southern Tibet: Implications for Indian slab dynamics, Geosphere, 12(4), 1198–1223, doi:10.1130/GES01325.1, 2016.

Lemcke, K.: Das Bayerische Alpenvorland vor der Eiszeit, Schweizerbart Science Publishers, Stuttgart, Germany., 1988.

Liniger, H.: Pliozän und Tektonik des Juragebirges, Eclogae Geol. Helv., 60(2), 407–490, 1967.

Lippitsch, R., Kissling, E. and Ansorge, J.: Upper mantle structure beneath the Alpine orogen from high-resolution teleseismic tomography, J. Geophys. Res., 108(B8), 2376, doi:10.1029/2002JB002016, 2003.

Madritsch, H., Schmid, S. M. and Fabbri, O.: Interactions between thin- and thick-skinned tectonics at the northwestern front of the Jura fold-and-thrust belt (eastern France), Tectonics, 27(5), TC5005, doi:10.1029/2008TC002282, 2008.

Mair, D., Lechmann, A., Herwegh, M., Nibourel, L. and Schlunegger, F.: Linking Alpine deformation in the Aar Massif basement and its cover units – the case of the Jungfrau–Eiger mountains (Central Alps, Switzerland), Solid Earth, 9(5), 1099–1122, doi:10.5194/se-9-1099-2018, 2018.

Mazurek, M., Hurford, A. J. and Leu, W.: Unravelling the multi-stage burial history of the Swiss Molasse Basin: integration of apatite fission track, vitrinite reflectance and biomarker isomerisation analysis, Basin Res., 18(1), 27–50, doi:10.1111/j.1365-2117.2006.00286.x, 2006.

Mitterbauer, U., Behm, M., Brückl, E., Lippitsch, R., Guterch, A., Keller, G. R., Koslovskaya, E., Rumpfhuber, E.-M. and Šumanovac, F.: Shape and origin of the East-Alpine slab constrained by the ALPASS teleseismic model, Tectonophysics, 510(1–2), 195–206, doi:10.1016/j.tecto.2011.07.001, 2011.

Mock, S. and Herwegh, M.: Tectonics of the central Swiss Molasse Basin: Post-Miocene transition to incipient thick-skinned tectonics?, Tectonics, 36(9), 1699–1723, doi:10.1002/2017TC004584, 2017.

Molnar, P., England, P. and Martinod, J.: Mantle dynamics, uplift of the Tibetan Plateau, and the Indian Monsoon, Rev. Geophys., 31(4), 357, doi:10.1029/93RG02030, 1993.

Mosar, J., Stampfli, G. M. and François, G.: Western Préalpes Médianes Romandes: Timing and structure. A review, Eclogae Geol. Helv., 89(1), 389–425, 1996.

Mosar, J.: Present-day and future tectonic underplating in the western Swiss Alps: reconciliation of basement/wrench-faulting and décollement folding of the Jura and Molasse basin in the Alpine foreland, Earth Planet. Sci. Lett., 173(3), 143–155, doi:10.1016/S0012-821X(99)00238-1, 1999.

Mosbrugger, V., Utescher, T. and Dilcher, D. L.: Cenozoic continental climatic evolution of Central Europe, Proc. Natl. Acad. Sci., 102(42), 14964–14969, doi:10.1073/pnas.0505267102, 2005.

Müller, M., Nieberding, F. and Wanninger, A.: Tectonic style and pressure distribution at the northern margin of the Alps between Lake Constance and the River Inn, Geol. Rundschau, 77(3), 787–796, doi:10.1007/BF01830185, 1988.

Nussbaum, C.: Neogene tectonics and thermal maturity of sediments of the easternmost Southern Alps (Friuli area, Italy), Université de Neuchâtel., 2000.

63

Oncken, O., Hindle, D., Kley, J., Elger, K., Victor, P. and Schemmann, K.: Deformation of the Central Andean Upper Plate System — Facts, Fiction, and Constraints for Plateau Models, in The Andes. Frontiers in Earth Sciences, edited by O. Oncken, G. Chong, G. Franz, P. Giese, H.-J. Götze, V. A. Ramos, M. R. Strecker, and P. Wigger, pp. 3–27, Springer, Berlin Heidelberg., 2006.

5   Ortner, H., Reiter, F. and Brandner, R.: Kinematics of the Inntal shear zone–sub-Tauern ramp fault system and the interpretation of the TRANSALP seismic section, Eastern Alps, Austria, Tectonophysics, 414(1–4), 241–258, doi:10.1016/j.tecto.2005.10.017, 2006.

Ortner, H., Aichholzer, S., Zerlauth, M., Pilser, R. and Fügenschuh, B.: Geometry, amount, and sequence of thrusting in the Subalpine Molasse of western Austria and southern Germany, European Alps, Tectonics, 34(1), 1–30, 10   doi:10.1002/2014TC003550, 2015.

Peresson, H. and Decker, K.: Far-field effects of Late Miocene subduction in the Eastern Carpathians: E-W compression and inversion of structures in the Alpine-Carpathian-Pannonian region, Tectonics, 16(1), 38–56, doi:10.1029/96TC02730, 1997.

Pfiffner, O. A.: Evolution of the North Alpine Foreland Basin in the Central Alps, in Foreland Basins, edited by P. A. Allen and P. Homewood, pp. 219–228, Blackwell Publishing Ltd., Oxford, UK., 1986.

15   Pfiffner, O. A.: Geologie der Alpen, 1st ed., Haupt, Bern, Stuttgart, Wien., 2009.

Pfiffner, O. A.: Structural Map of the Helvetic Zone of the Swiss Alps, including Vorarlberg (Austria) and Haute Savoie (France), 1:100 000, edited by Federal Office of Topography swisstopo, Geol. Spec. Map, 128(Explanatory notes), 2011.

Pfiffner, O. A., Erard, P. F. and Stäuble, M.: Two cross sections through the Swiss Molasse Basin (lines E4-E6, W1, W7-W10), in Deep structure of the Swiss Alps. Results of NRP 20, edited by O. A. Pfiffner, P. Lehner, P. Heitzmann, S. Mueller, 20   and A. Steck, pp. 64–72, Birkhäuser, Basel, Boston, Berlin., 1997.

Philippe, Y., Colletta, B., Deville, E. and Mascle, A.: The Jura fold-and-thrust belt: a kinematic model based on map-balancing, in Peri Thetys Memoir 2: Structure and prospects of Alpine Basins and Forelands, edited by P. A. Ziegler and F. Horvàth, pp. 235–261, Muséum national d'Histoire naturelle, Paris., 1996.

Pippèrr, M. and Reichenbacher, B.: Late Early Miocene palaeoenvironmental changes in the North Alpine Foreland Basin, 25   Palaeogeogr. Palaeoclimatol. Palaeoecol., 468, 485–502, doi:10.1016/j.palaeo.2017.01.002, 2017.

Qorbani, E., Bianchi, I. and Bokelmann, G.: Slab detachment under the Eastern Alps seen by seismic anisotropy, Earth Planet. Sci. Lett., 409, 96–108, doi:10.1016/j.epsl.2014.10.049, 2015.

Ratschbacher, L., Frisch, W., Linzer, H.-G. and Merle, O.: Lateral extrusion in the eastern Alps, PArt 2: Structural analysis, Tectonics, 10(2), 257–271, doi:10.1029/90TC02623, 1991.

Reiners, P. W. and Brandon, M. T.: Using Thermochronology to Understand Orogenic Erosion, Annu. Rev. Earth Planet. Sci., 34(1), 419–466, doi:10.1146/annurev.earth.34.031405.125202, 2006.

Rosenberg, C. L. and Berger, A.: On the causes and modes of exhumation and lateral growth of the Alps, Tectonics, 28(6), TC6001, doi:10.1029/2008TC002442, 2009.

5 Rosenberg, C. L. and Kissling, E.: Three-dimensional insight into Central-Alpine collision: Lower-plate or upper-plate indentation?, Geology, 41(12), 1219–1222, doi:10.1130/G34584.1, 2013.

Rosenberg, C. L., Berger, A., Bellahsen, N. and Bousquet, R.: Relating orogen width to shortening, erosion, and exhumation during Alpine collision, Tectonics, 34(6), 1306–1328, doi:10.1002/2014TC003736, 2015.

Rosenberg, C. L., Schneider, S., Scharf, A., Bertrand, A., Hammerschmidt, K., Rabaute, A. and Brun, J.-P.: Relating collisional

10 kinematics to exhumation processes in the Eastern Alps, Earth-Science Rev., 176(October 2017), 311–344, doi:10.1016/j.earscirev.2017.10.013, 2018.

Rutsch, R.: Molasse und Quartär im Gebiet des Siegfriedblattes Rüeggisberg (Kanton Bern), Beiträge zur Geol. Karte der Schweiz, NF 87, 89 pp., 1947.

Schegg, R. and Leu, W.: Analysis of erosion events and palaeogeothermal gradients in the North Alpine Foreland Basin of

15 Switzerland, Geol. Soc. London, Spec. Publ., 141(1), 137–155, doi:10.1144/GSL.SP.1998.141.01.09, 1998.

Schlunegger, F. and Castelltort, S.: Immediate and delayed signal of slab breakoff in Oligo/Miocene Molasse deposits from the European Alps, Sci. Rep., 6, 31010, doi:10.1038/srep31010, 2016.

Schlunegger, F. and Kissling, E.: Slab rollback orogeny in the Alps and evolution of the Swiss Molasse basin, Nat. Commun., 6, 8605, doi:10.1038/ncomms9605, 2015.

20 Schlunegger, F. and Mosar, J.: The last erosional stage of the Molasse Basin and the Alps, Int. J. Earth Sci., 100(5), 1147–1162, doi:10.1007/s00531-010-0607-1, 2011.

Schlunegger, F. and Norton, K. P.: Headward retreat of streams in the Late Oligocene to Early Miocene Swiss Alps, edited by K. Föllmi, Sedimentology, 60(1), 85–101, doi:10.1111/sed.12010, 2013.

Schlunegger, F. and Norton, K. P.: Climate vs. tectonics: the competing roles of Late Oligocene warming and Alpine

25 orogenesis in constructing alluvial megafan sequences in the North Alpine foreland basin, Basin Res., 27(2), 230–245, doi:10.1111/bre.12070, 2015.

Schlunegger, F. and Simpson, G.: Possible erosional control on lateral growth of the European Central Alps, Geology, 30(10), 907, doi:10.1130/0091-7613(2002)030<0907:PECOLG>2.0.CO;2, 2002.

Schlunegger, F., Matter, A. and Mange, M. A.: Alluvial fan sedimentation and structure of the southern Molasse Basin margin,

Lake Thun area, Switzerland, Eclogae Geol. Helv., 86(3), 717–750, 1993.

Schlunegger, F., Burbank, D. W., Matter, A., Engesser, B. and Mödden, C.: Magnetostratigraphic calibration of the Oligocence to Middle Miocene (30-15 Ma) mammal biozones and depositional sequences of the Swiss Molasse Basin, Eclogae Geol. Helv., 89, 753–788, 1996.

5   Schlunegger, F., Matter, A., Burbank, D. W. and Klaper, E. M.: Magnetostratigraphic constraints on relationships between evolution of the central Swiss Molasse basin and Alpine orogenic events, Geol. Soc. Am. Bull., 109(2), 225–241, doi:10.1130/0016-7606(1997)109<0225:MCORBE>2.3.CO;2, 1997.

Schlunegger, F., Rieke-Zapp, D. and Ramseyer, K.: Possible environmental effects on the evolution of the Alps-Molasse Basin system, Swiss J. Geosci., 100(3), 383–405, doi:10.1007/s00015-007-1238-9, 2007.

10   Schlunegger, F., Anspach, O., Bieri, B., Böning, P., Kaufmann, Y., Lahl, K., Lonschinski, M., Mollet, H., Sachse, D., Schubert, C., Stöckli, G. and Zander, I.: Geological Atlas of Switzerland 1:25000, Map sheet Schüpfheim (LK 1169), Federal Office of Topography swisstopo, Wabern, Switzerland., 2016.

Schmid, S. M., Pfiffner, O. A., Froitzheim, N., Schönborn, G. and Kissling, E.: Geophysical-geological transect and tectonic evolution of the Swiss-Italian Alps, Tectonics, 15(5), 1036–1064, doi:10.1029/96TC00433, 1996.

15   Schmid, S. M., Fügenschuh, B., Kissling, E. and Schuster, R.: Tectonic map and overall architecture of the Alpine orogen, Eclogae Geol. Helv., 97(1), 93–117, doi:10.1007/s00015-004-1113-x, 2004.

Schmid, S. M., Kissling, E., Diehl, T., van Hinsbergen, D. J. J. and Molli, G.: Ivrea mantle wedge, arc of the Western Alps, and kinematic evolution of the Alps–Apennines orogenic system, Swiss J. Geosci., 110(2), 581–612, doi:10.1007/s00015-016-0237-0, 2017.

20   Schönborn, G.: Alpine tectonics and kinematic models of the central Southern Alps, Mem. di Sci. Geol. Padova, 44, 229–393, 1992.

Schuller, V., Frisch, W. and Herzog, U.: Critical taper behaviour and out-of-sequence thrusting on orogenic wedges - an example of the Eastern Alpine Molasse Basin, Terra Nov., 27(3), 231–237, doi:10.1111/ter.12152, 2015.

~~Schwartz, S., Gautheron, C., Audin, L., Dumont, T., Nomade, J., Barbarand, J., Pinna-Jamme, R. and van der Beek, P.:~~
25 ~~Foreland exhumation controlled by crustal thickening in the Western Alps, Geology, 45(2), 139–142, doi:10.1130/G38561.1,~~
~~2017.~~

Sinclair, H. D.: Flysch to molasse transition in peripheral foreland basins: The role of the passive margin versus slab breakoff, Geology, 25(12), 1123, doi:10.1130/0091-7613(1997)025<1123:FTMTIP>2.3.CO;2, 1997.

Sinclair, H. D. and Allen, P. A.: Vertical versus horizontal motions in the Alpine orogenic wedge: stratigraphic response in the

foreland basin, Basin Res., 4(3–4), 215–232, doi:10.1111/j.1365-2117.1992.tb00046.x, 1992.

Sinclair, H. D., Coakley, B. J., Allen, P. A. and Watts, A. B.: Simulation of Foreland Basin Stratigraphy using a diffusion model of mountain belt uplift and erosion: An example from the central Alps, Switzerland, Tectonics, 10(3), 599–620, doi:10.1029/90TC02507, 1991.

5 Sommaruga, A.: Décollement tectonics in the Jura forelandfold-and-thrust belt, Mar. Pet. Geol., 16(2), 111–134, doi:10.1016/S0264-8172(98)00068-3, 1999.

Sommaruga, A., Eichenberger, U. and Marillier, F.: Seismic Atlas of the Swiss Molasse Basin, edited by the Swiss Geophysical Commission, Matériaux pour la Géologie la Suisse - Géophysique, (44), 2012.

Spiegel, C., Kuhlemann, J., Dunkl, I. and Frisch, W.: Paleogeography and catchment evolution in a mobile orogenic belt: the
10 Central Alps in Oligo–Miocene times, Tectonophysics, 341(1–4), 33–47, doi:10.1016/S0040-1951(01)00187-1, 2001.

Stampfli, G. M. and Marchant, R. H.: Geodynamic evolution of the Tethyan margins of the Western Alps, in Deep structure of the Swiss Alps: Results of NRP 20, edited by O. A. Pfiffner, P. Lehner, P. Heitzmann, S. Mueller, and A. Steck, pp. 223–240, Birkhäuser, Basel, Boston, Berlin., 1997.

Stäuble, M. and Pfiffner, O. A.: Processing, interpretation and modeling of seismic reflection data in the Molasse Basin of
15 eastern Switzerland, Eclogae Geol. Helv., 84(1), 151–175, doi:10.5169/seals-166767, 1991.

Strunck, P. and Matter, A.: Depositional evolution of the western Swiss Molasse, Eclogae Geol. Helv., 95(2), 197–222, doi:http://dx.doi.org/10.5169/seals-168955, 2002.

Todd, C. S. and Engi, M.: Metamorphic field gradients in the Central Alps, J. Metamorph. Geol., 15(4), 513–530, doi:10.1111/j.1525-1314.1997.00038.x, 1997.

20 Ustaszewski, K. and Schmid, S. M.: Latest Pliocene to recent thick-skinned tectonics at the Upper Rhine Graben – Jura Mountains junction, Swiss J. Geosci., 100(2), 293–312, doi:10.1007/s00015-007-1226-0, 2007.

Valla, P. G., van der Beek, P. A., Shuster, D. L., Braun, J., Herman, F., Tassan-Got, L. and Gautheron, C.: Late Neogene exhumation and relief development of the Aar and Aiguilles Rouges massifs (Swiss Alps) from low-temperature thermochronology modeling and 4 He/ 3 He thermochronometry, J. Geophys. Res. Earth Surf., 117, F01004,
25 doi:10.1029/2011JF002043, 2012.

Vermeesch, P.: Three new ways to calculate average (U–Th)/He ages, Chem. Geol., 249(3–4), 339–347, doi:10.1016/j.chemgeo.2008.01.027, 2008.

Vernon, A. J., van der Beek, P. A., Sinclair, H. D., Persano, C., Foeken, J. and Stuart, F. M.: Variable late Neogene exhumation of the central European Alps: Low-temperature thermochronology from the Aar Massif, Switzerland, and the Lepontine Dome,

Italy, Tectonics, 28(5), TC5004, doi:10.1029/2008TC002387, 2009.

Vollmayr, T.: Strukturelle Ergebnisse der Kohlenwasserstoffexploration im Gebiet von Thun, Schweiz, Eclogae Geol. Helv., 85(3), 531–539, 1992.

Wehrens, P., Baumberger, R., Berger, A. and Herwegh, M.: How is strain localized in a meta-granitoid, mid-crustal basement section? Spatial distribution of deformation in the central Aar massif (Switzerland), J. Struct. Geol., 94, 47–67, doi:10.1016/j.jsg.2016.11.004, 2017.

Weidmann, M., Homewood, P., Morel, R., Berchten, J.-D., Bucher, H., Burri, M., Cornioley, J.-D., Escher, P., Rück, P., Tabotta, A. and Zahner, P.: Geological Atlas of Switzerland 1:25000, Map sheet Châtel-St-Denis (LK 1244), Federal Office of Topography swisstopo, Wabern, Switzerland., 1993.

Weisenberger, T. B., Rahn, M. K., van der Lelij, R., Spikings, R. A. and Bucher, K.: Timing of low-temperature mineral formation during exhumation and cooling in the Central Alps, Switzerland, Earth Planet. Sci. Lett., 327–328, 1–8, doi:10.1016/j.epsl.2012.01.007, 2012.

Whipple, K. X.: The influence of climate on the tectonic evolution of mountain belts, Nat. Geosci., 2(2), 97–104, doi:10.1038/ngeo413, 2009.

Willett, S. D. and Schlunegger, F.: The last phase of deposition in the Swiss Molasse Basin: from foredeep to negative-alpha basin, Basin Res., 22(5), 623–639, doi:10.1111/j.1365-2117.2009.00435.x, 2010.

Willett, S. D., Schlunegger, F. and Picotti, V.: Messinian climate change and erosional destruction of the central European Alps, Geology, 34(8), 613, doi:10.1130/G22280.1, 2006.

Wolf, R. A., Farley, K. A. and Silver, L. T.: Helium diffusion and low-temperature thermochronometry of apatite, Geochim. Cosmochim. Acta, 60(21), 4231–4240, doi:10.1016/S0016-7037(96)00192-5, 1996.

Zaugg, A., Löpfe, R., Kriemler, M. and Kempf, T.: Geological Atlas of Switzerland 1:25000, Federal Office of Topography swisstopo, Wabern, Switzerland., 2011.

Zhao, L., Paul, A., Malusà, M. G., Xu, X., Zheng, T., Solarino, S., Guillot, S., Schwartz, S., Dumont, T., Salimbeni, S., Aubert, C., Pondrelli, S., Wang, Q. and Zhu, R.: Continuity of the Alpine slab unraveled by high-resolution P wave tomography, J. Geophys. Res. Solid Earth, 121(12), 8720–8737, doi:10.1002/2016JB013310, 2016.

Zweigel, J., Aigner, T., Luterbacher, H., Fleet, A. J., Morton, A. C. and Roberts, A. M.: Eustatic versus tectonic controls on Alpine foreland basin fill: sequence stratigraphy and subsidence analysis in the SE German molasse, Cenozoic Forel. basins West. Eur., 134, 299–324, doi:10.1144/GSL.SP.1998.134.01.14, 1998.

Sample	He vol. [ncc][a]	1σ [%]	U mass [ng]	1σ [%]	Th mass [ng]	1σ [%]	Sm mass [ng]	1σ [%]	Ft[b]	Raw age [Ma]	Corrected age [Ma]	2σ [Ma][c]	Average age [Ma][d]	2 std. error [Ma][e]	Excluded age[f]
SM-1 a1	0.02	3.77	0.01	5.64	0.07	2.56	0.34	7.06	0.60	5.5	9.0	1.4			
SM-1 a2	0.08	2.09	0.04	2.66	0.21	2.45	0.98	6.92	0.72	7.2	10.0	1.0			
SM-1 a4	0.07	2.43	0.03	3.18	0.15	2.47	0.66	6.84	0.74	8.5	11.5	1.2			
SM-1 a5	0.03	3.70	0.02	4.97	0.07	2.56	0.40	7.15	0.69	6.2	9.0	1.2			
SM-1 a6	0.08	2.09	0.03	2.52	0.15	2.45	0.55	3.47	0.68	9.4	13.9	1.5			
SM-1 a7	0.05	2.67	0.02	3.25	0.14	2.46	0.92	3.64	0.79	6.9	8.8	0.8			
SM-1 a8	0.04	3.24	0.03	2.65	0.02	2.82	0.23	3.34	0.64	8.1	12.6	1.7	10.7	0.8	
SM-4 a1	0.03	3.13	0.02	3.08	0.01	2.48	0.03	3.70	0.66	10.5	15.9	2.1			e
SM-4 a2	0.06	2.51	0.06	2.03	0.10	2.42	0.37	3.70	0.61	5.9	9.6	1.2			
SM-4 a3	0.01	4.81	0.02	3.79	0.05	2.49	0.56	3.70	0.59	3.0	5.0	0.8			e
SM-4 a4	0.06	2.64	0.05	2.20	0.06	2.45	0.51	3.70	0.61	6.6	10.8	1.4			
SM-4 a5	0.02	4.31	0.02	3.99	0.03	2.54	0.34	3.70	0.55	5.0	9.2	1.5			
SM-4 a6	0.08	2.21	0.07	2.01	0.02	2.64	0.38	3.70	0.66	8.6	13.1	1.5	10.7	0.9	
SM-5 a1	0.05	2.79	0.04	2.52	0.13	2.46	0.90	3.70	0.62	4.7	7.5	1.0			
SM-5 a2	0.10	2.11	0.15	1.86	0.09	2.43	0.66	3.70	0.66	4.6	7.0	0.8			
SM-5 a3	0.02	4.42	0.02	4.25	0.06	2.57	0.25	3.70	0.74	4.3	5.8	0.7			
SM-5 a4	0.01	5.90	0.01	6.10	0.09	2.50	0.22	3.70	0.62	2.2	3.6	0.6			e
SM-5 a5	0.04	3.02	0.04	2.35	0.15	2.46	1.00	3.70	0.65	3.7	5.6	0.7			
SM-5 a6	0.20	1.51	0.13	1.88	0.08	2.44	0.54	3.70	0.63	11.3	18.1	2.2	6.5	0.5	e
SM-6 a1	0.05	2.66	0.05	2.20	0.10	2.43	0.83	3.70	0.61	6.0	9.8	1.3			
SM-6 a2	0.07	2.20	0.07	2.04	0.12	2.47	1.30	3.70	0.82	5.6	6.8	0.5			
SM-6 a3	0.04	2.90	0.04	2.29	0.08	2.44	0.77	3.70	0.61	4.8	7.8	1.1			
SM-6 a4	0.00	9.84	0.00	43.45	0.01	2.77	1.05	3.70	0.59	0.8	1.3	0.4			e
SM-6 a5	0.14	1.72	0.13	1.87	0.02	2.68	0.51	3.70	0.64	7.9	12.3	1.4	9.2	1.2	
SM-7 a1	0.01	7.55	0.01	5.93	0.03	2.67	0.34	4.55	0.54	2.1	3.9	0.8			e
SM-7 a2	0.03	3.57	0.02	3.57	0.02	2.88	0.43	3.21	0.69	7.9	11.5	1.5			
SM-7 a3	0.15	1.66	0.07	2.00	0.07	2.52	0.31	4.06	0.62	13.5	21.7	2.7			
SM-7 a4	0.02	4.43	0.02	4.16	0.04	2.62	0.31	3.52	0.57	5.1	9.0	1.5			
SM-7 a5	0.05	2.85	0.03	2.82	0.05	2.58	0.41	3.81	0.54	8.4	15.7	2.4			
SM-7 a6	0.02	4.37	0.02	3.98	0.05	2.45	0.57	3.70	0.71	3.7	5.2	0.7			e
SM-7 a7	0.02	4.28	0.01	6.31	0.04	2.65	0.60	3.70	0.65	6.1	9.5	1.4			
SM-7 a8	0.24	1.48	0.13	1.87	0.11	2.42	0.57	3.70	0.73	12.3	16.9	1.6			
SM-7 a9	0.00	8.62	0.00	28.40	0.03	2.69	0.30	3.70	0.55	2.4	4.3	1.1			e
SM-8 a1	0.02	3.67	0.02	3.39	0.06	2.54	0.56	4.01	0.77	4.4	5.7	0.6			
SM-8 a2	0.02	3.68	0.03	3.02	0.03	2.67	0.43	4.57	0.70	4.7	6.8	0.8			
SM-8 a3	0.12	1.93	0.03	2.61	0.08	2.50	0.56	3.86	0.77	18.5	24.0	2.1			e
SM-8 a4	0.02	3.88	0.02	3.25	0.06	2.55	0.53	3.32	0.80	4.5	5.6	0.6	6.0	0.4	
SM-11 a1	0.05	2.53	0.05	2.14	0.11	2.42	0.47	4.56	0.78	5.5	7.0	0.6			
SM-11 a2	0.02	4.35	0.02	3.89	0.06	2.45	0.34	3.42	0.73	5.3	7.2	0.9			
SM-11 a3	0.02	4.04	0.02	4.02	0.07	2.43	0.52	3.68	0.75	4.1	5.6	0.7			
SM-11 a4	0.02	4.77	0.02	3.77	0.06	2.44	0.30	4.20	0.57	3.8	6.6	1.1			
SM-11 a5	0.05	2.52	0.04	2.35	0.04	2.49	0.26	4.54	0.67	9.2	13.6	1.6	6.6	0.4	e
SM-12 a1	0.04	3.00	0.04	2.22	0.06	2.44	0.40	3.80	0.51	5.5	10.7	1.7			
SM-12 a2	0.26	1.50	0.15	1.84	0.01	2.72	0.46	4.13	0.69	13.4	19.4	2.0			e
SM-12 a3	0.02	3.63	0.03	2.85	0.03	2.51	0.36	3.46	0.74	5.4	7.3	0.8			
SM-12 a4	0.22	1.50	0.19	1.83	0.18	2.41	0.46	4.07	0.82	7.8	9.6	0.7	9.2	1.0	
SM-13 a1	0.06	2.27	0.07	1.99	0.02	2.84	0.59	3.13	0.61	6.1	10.0	1.3			

Sample	He vol. [ncc][a]	1σ [%]	U mass [ng]	1σ [%]	Th mass [ng]	1σ [%]	Sm mass [ng]	1σ [%]	Ft[b]	Raw age [Ma]	Corrected age [Ma]	2σ [Ma][c]	Average age [Ma][d]	2 std. error [Ma][e]	Excluded age[f]
SM-13 a2	0.04	2.93	0.03	2.54	0.04	2.67	0.39	3.93	0.68	6.6	9.7	1.2			
SM-13 a3	0.06	2.59	0.07	2.05	0.01	3.46	0.35	4.68	0.74	6.8	9.1	0.9			
SM-13 a4	0.02	4.51	0.02	2.96	0.02	2.71	0.31	4.28	0.63	4.3	6.9	1.0			
SM-13 a5	0.01	6.37	0.01	5.91	0.01	2.82	0.34	3.96	0.76	3.2	4.2	0.7	8.9	0.7	e
SM-14 a1	0.06	2.60	0.03	2.71	0.06	2.44	0.55	3.70	0.68	8.9	13.0	1.5			e
SM-14 a2	0.03	3.33	0.02	3.21	0.07	2.44	0.39	3.70	0.56	6.4	11.4	1.7			
SM-14 a3	0.05	2.66	0.03	2.70	0.10	2.48	0.32	3.70	0.59	6.8	11.4	1.6			
SM-14 a4	0.02	4.41	0.02	3.66	0.05	2.62	1.11	3.70	0.61	3.4	5.7	0.9			e
SM-14 a5	0.04	3.07	0.02	3.59	0.07	2.53	0.41	3.70	0.73	7.1	9.7	1.1			
SM-14 a6	0.07	2.25	0.05	2.10	0.09	2.43	2.20	3.70	0.79	6.5	8.3	0.7	10.8	0.6	e
SM-15 a1	0.04	2.72	0.04	2.44	0.18	2.41	2.39	3.70	0.71	3.5	5.0	0.5			
SM-15 a2	0.11	1.82	0.05	2.33	0.12	2.42	0.39	3.70	0.66	12.2	18.4	2.1			e
SM-15 a3	0.04	2.92	0.04	2.60	0.17	2.41	0.82	3.70	0.64	3.7	5.8	0.7			
SM-15 a4	0.46	1.26	0.16	1.85	0.77	2.41	0.62	3.70	0.76	11.1	14.5	1.2			e
SM-15 a5	0.03	3.24	0.03	2.87	0.08	2.50	0.51	3.70	0.61	4.0	6.5	0.9			
SM-15 a6	0.08	2.13	0.07	2.16	0.17	2.42	2.56	3.70	0.69	4.8	7.0	0.8	6.1	0.4	
SM-16 a1	0.27	1.33	0.09	1.96	0.09	2.43	3.15	3.70	0.71	16.6	23.5	2.3			
SM-16 a2	0.90	1.01	0.36	1.82	0.28	2.41	1.98	3.70	0.73	16.9	23.2	2.1			
SM-16 a3	0.25	1.56	0.12	1.87	0.18	2.41	0.37	3.70	0.72	12.5	17.3	1.6			e
SM-16 a4	0.01	6.40	0.01	7.86	0.06	2.46	0.28	3.70	0.75	3.3	4.3	0.7			e
SM-16 a5	0.14	1.77	0.18	1.84	0.03	2.52	1.03	3.70	0.76	6.0	7.9	0.7			
SM-16 a7	0.04	3.25	0.09	1.90	0.07	2.44	0.55	3.70	0.69	3.1	4.4	0.5			e

[a] Amount of helium is given in nano-cubic-cm in standard temperature and pressure.

[b] Ejection correction (Ft): correction factor for alpha-ejection (Farley et al., 1996; Hourigan et al., 2005).

[c] Uncertaintiy of the single grain age is given as 2 sigma in % (or in Ma) and it includs both the analytical uncertainty and the estimated uncertainty of the Ft.

[d] Average ages for totally reset samples were calculated as the unweighted arithmetic mean.

[g] Uncertainty of the sample average age is 2 standard error, as (SD)/(n)1/2; where SD=standard deviation of the age replicates and n=number of age determinations.

[f] Ages with a substantial first He re-extract (>4%) and/or a total analytical error of >10% have been excluded. Outliers on the [He]–P plot have also been excluded (Vermeesch, 2008).
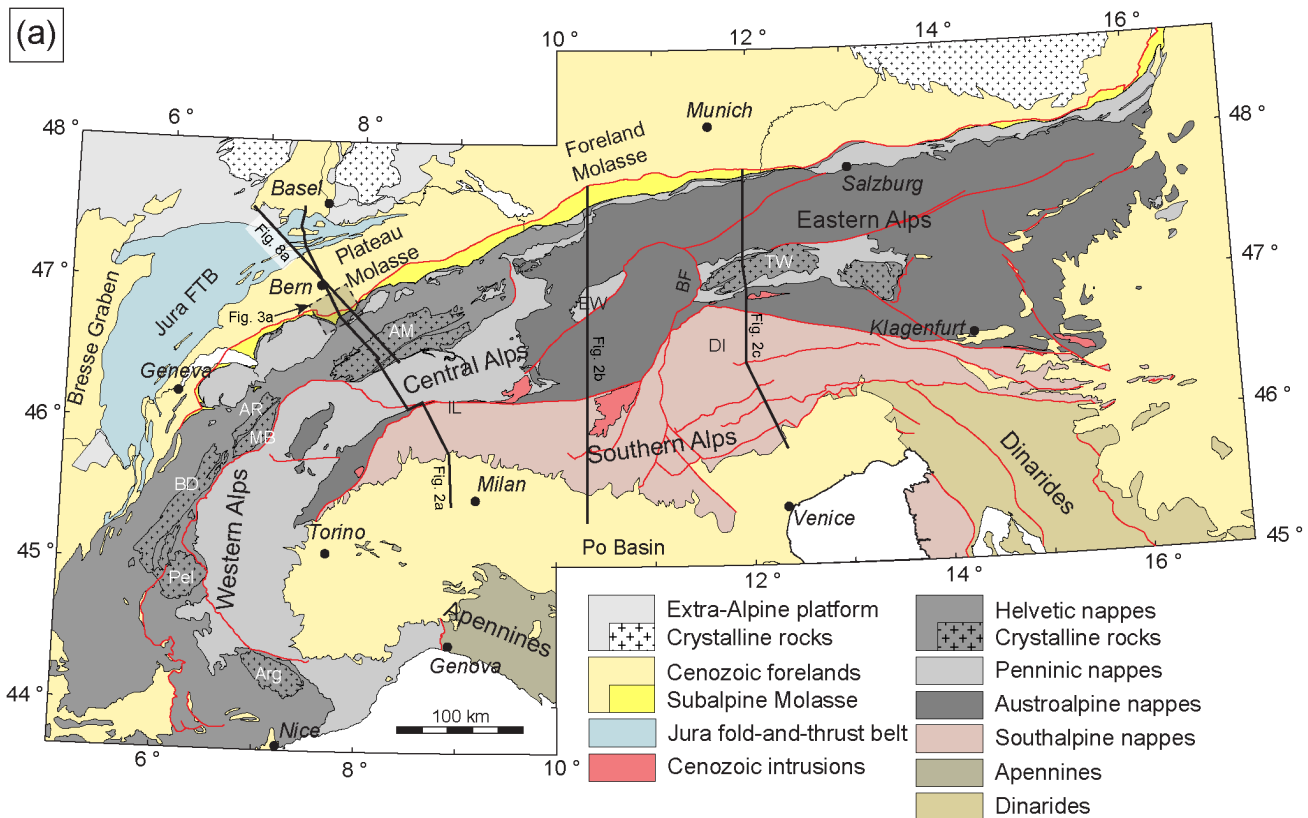
Fig. 1 (a) Tectonic map of the European Alps and its foreland basins (adapted from Schmid et al., 2004). Traces of the cross-sections in Fig. 2 and Fig. 8a are given as bold black lines. The sample area south of Bern (Fig. 3a) is denoted by a dashed rectangle. AM, Aar Massif; AR, Aiguilles-Rouges Massif; BD, Belledonne Massif; BF, Brenner Fault; DI, Dolomite indenter; EW, Engadine Window; FTB, fold-and-thrust belt; IL, Insubric Line; MB, Mont-Blanc Massif; Pel, Pelvoux Massif; TW, Tauern Window

71
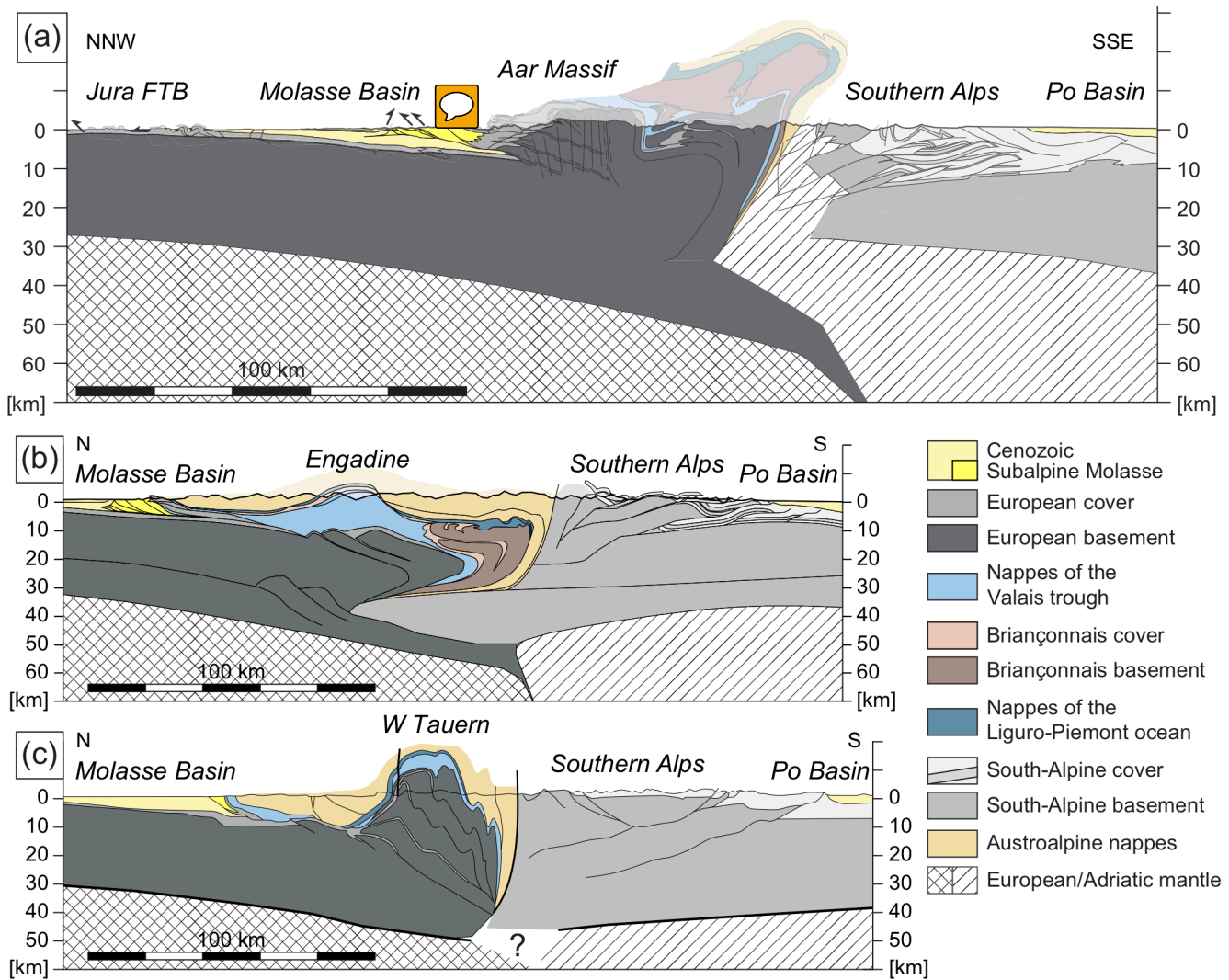
Fig. 2 Cross-sections through the Alps. (a) Jura - Plateau Molasse - Aar Massif (compiled from Buxtorf, 1916; Herwegh et al., 2017; Mock and Herwegh, 2017; Pfiffner, 2009; Rosenberg and Kissling, 2013). (b) Engadine Window (adapted from Rosenberg et al., 2015). (c) Western Tauern Window (adapted from Rosenberg et al., 2015).
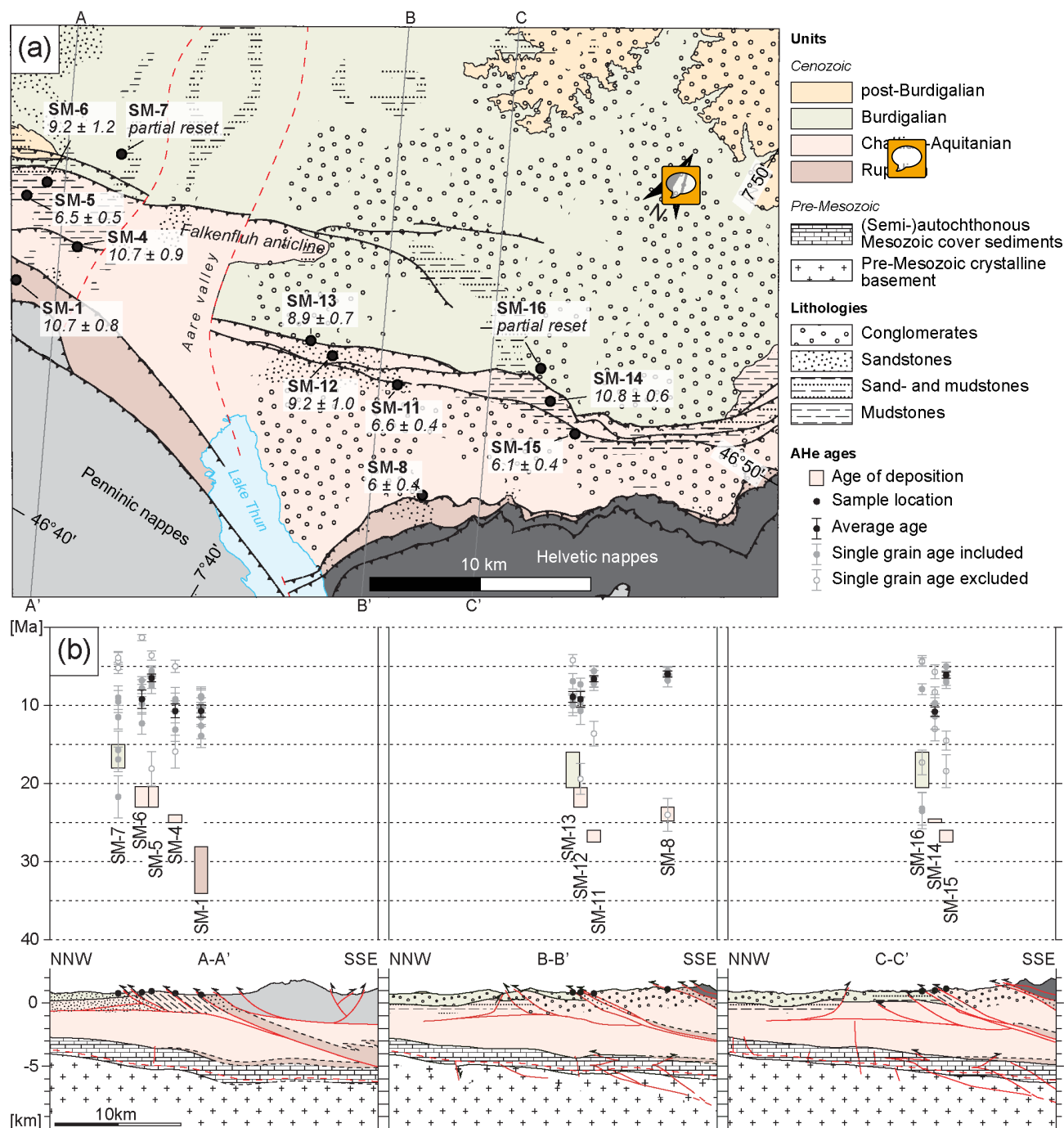
Fig. 3 (a) Litho-tectonic map of the Lake Thun area showing sample locations and corresponding average apatite (U-Th-Sm)/He (AHe) ages. Traces of cross-sections A-A', B-B', and C-C' in Fig. 3b are given as black lines. The location of the sampling area is shown as a dashed rectangle in Fig. 1. Note the arrow indicating north. (b) Cross-sections through the sampling area west (A-A') and east of the Aare valley (B-B' and C-C'), showing single grain and average AHe ages

Post-depositional cooling history

Envelope of acceptable paths (goodness of-fit ≥ 0.05)

Good paths (goodness of-fit ≥ 0.5)

Thrust
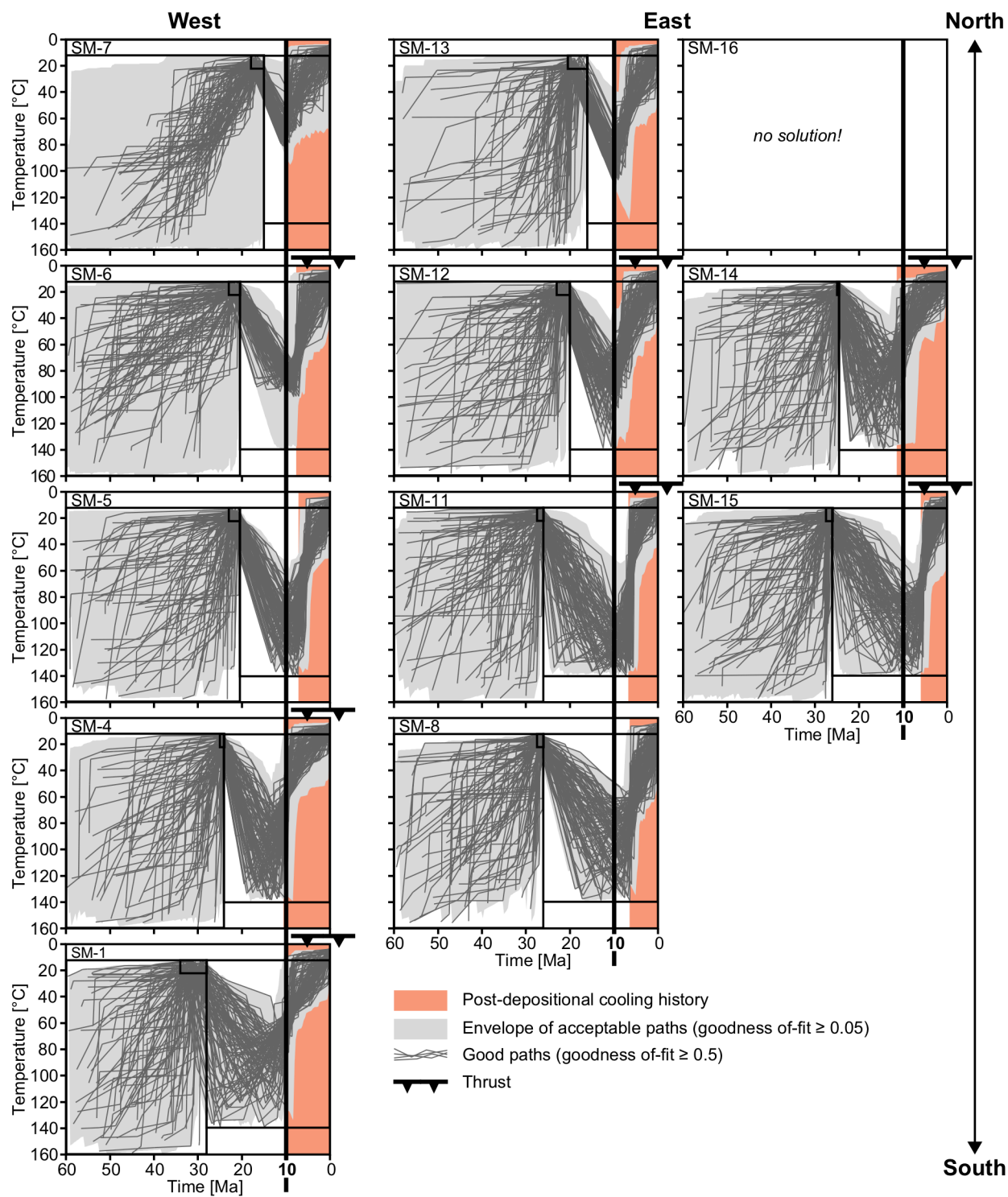
Fig. 4 Thermal evolution of samples. The results from inverse modeling of apatite (U-Th-Sm)/He (AHe) ages with the HeFTy software (Ketcham, 2005) show the time-temperature history of the samples discussed in the text. Modeling constraints are shown as black boxes. The bold black lines at 10 Ma serve as a visual time reference. The thermal histories for the different samples are aligned from north to south and from east to west according to their sample location
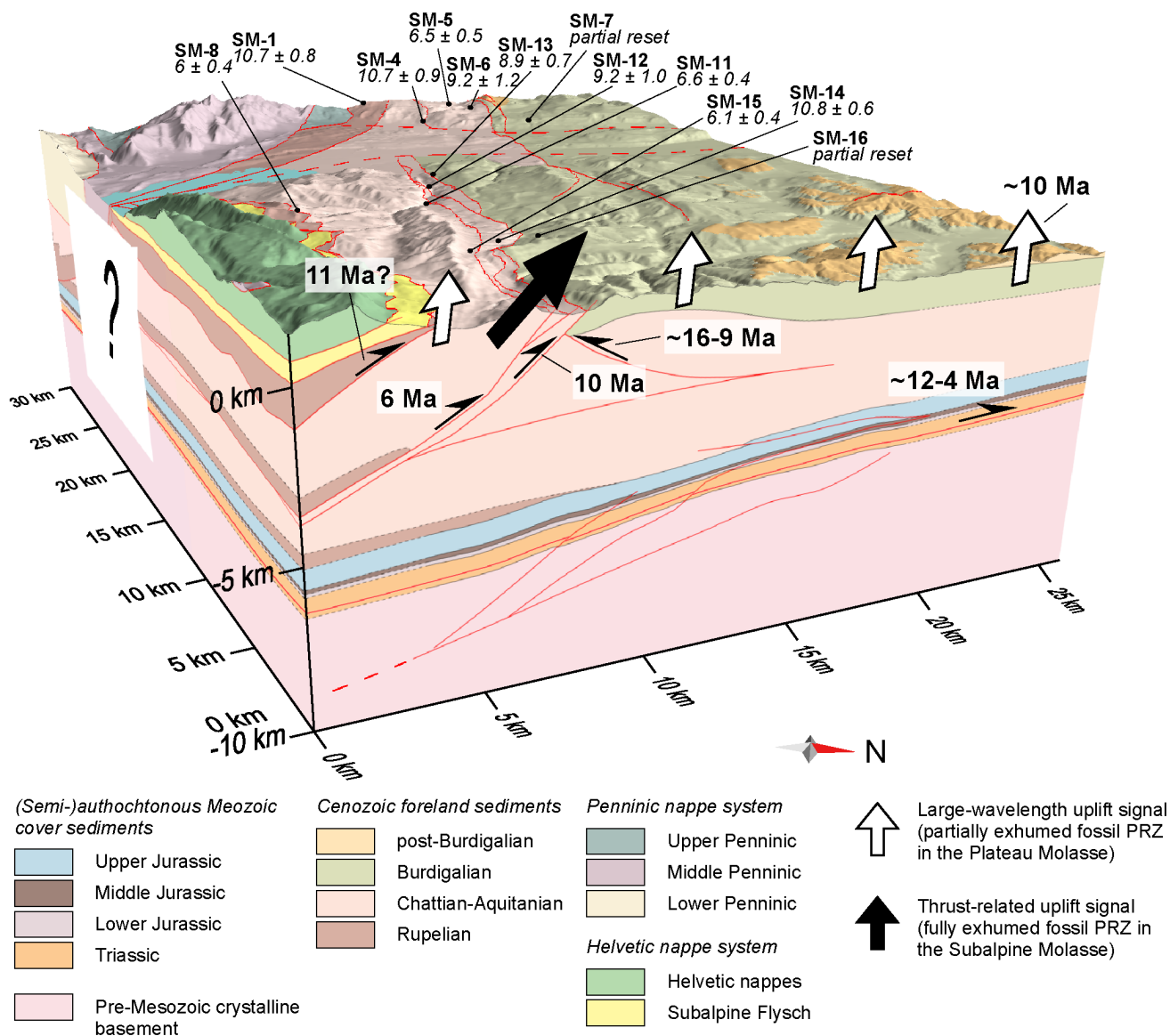
Fig. 5 Block model of with sample locations and corresponding average (U-Th-Sm)/He ages. The construction of the block model is based on surface (Beck, 1945; Haus, 1937; Jordi, 2012; Rutsch, 1947; Schlunegger et al., 1993, 1997) and subsurface (2D seismic interpretation; Mock and Herwegh, 2017) geological information. PRZ, partial retention zone

Fig. 6 Along-strike variations in late Miocene deformation of the North Alpine foreland between Lake Geneva and Salzburg. (a) Tectonic map (modified from Schmid et al., 2004) and activity of thrusting in the Subalpine Molasse deduced from AHe ages and geological interpretation. (b) Tectonic map (modified from Schmid et al., 2004) and estimated amount of late Miocene shortening in the North Alpine foreland (i.e., Subalpine Molasse, and Jura FTB). Estimates from the Subalpine Molasse record minimum shortening. (c) Top basement map of the Central Alps (modified from Pfiffner, 2011) showing the highly non-cylindrical hinterland architecture with the high relief domains of the External Crystalline Massifs (ECMs). Red arrows indicate the constant late Miocene deformation signal with a slight decrease in horizontal shortening recorded in the North Alpine foreland. AM, Aar Massif; AR, Aiguilles-Rouges Massif; BD, Belledonne Massif; EW, Engadine Window; MB, Mont-Blanc Massif; TW, Tauern Window
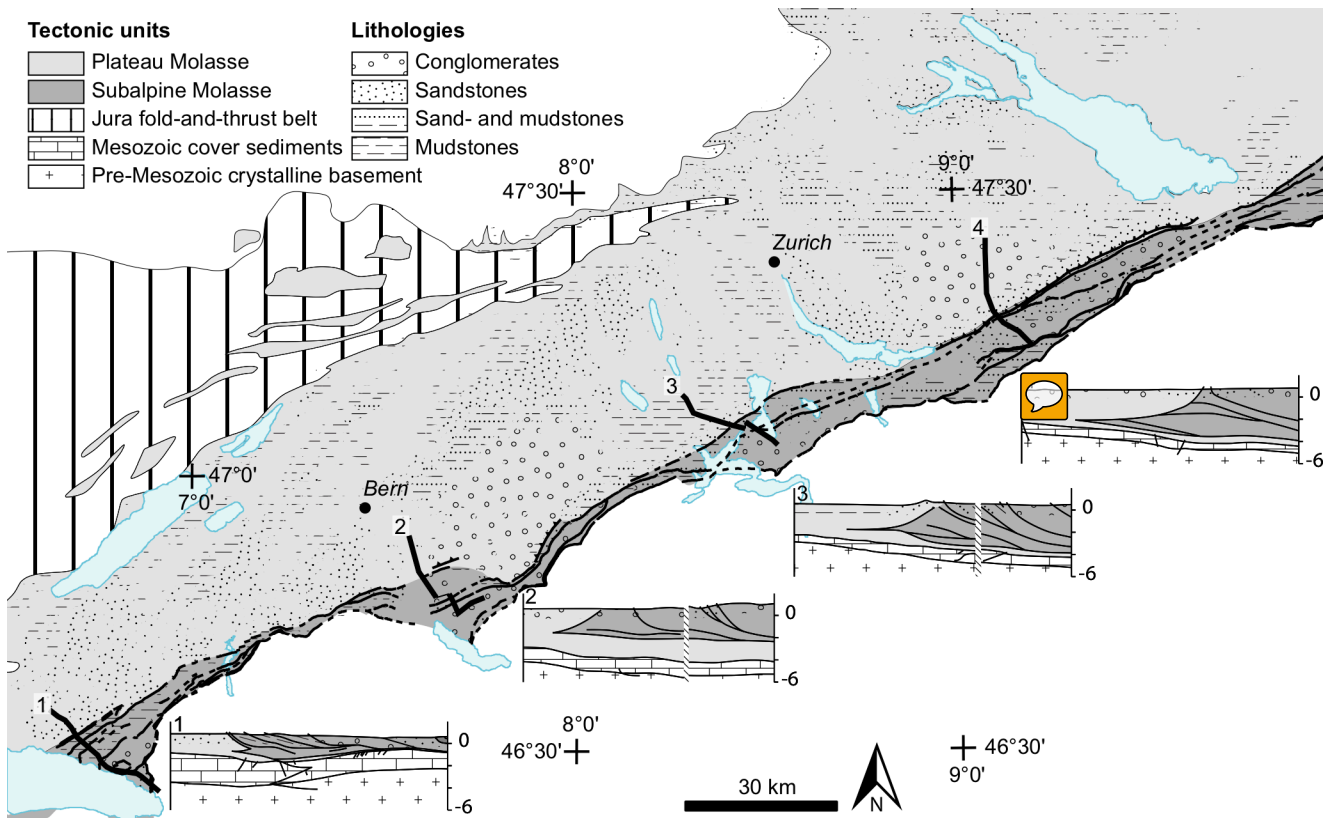
Fig. 7 Litho-tectonic map of the Swiss Molasse Basin (modified from Landesgeologie, 2005). Cross-sections 1-4 are based on 2D seismic interpretation (cross-section 2, Mock and Herwegh, 2017; cross-sections 1, 3, and 4, Sommaruga et al., 2012)
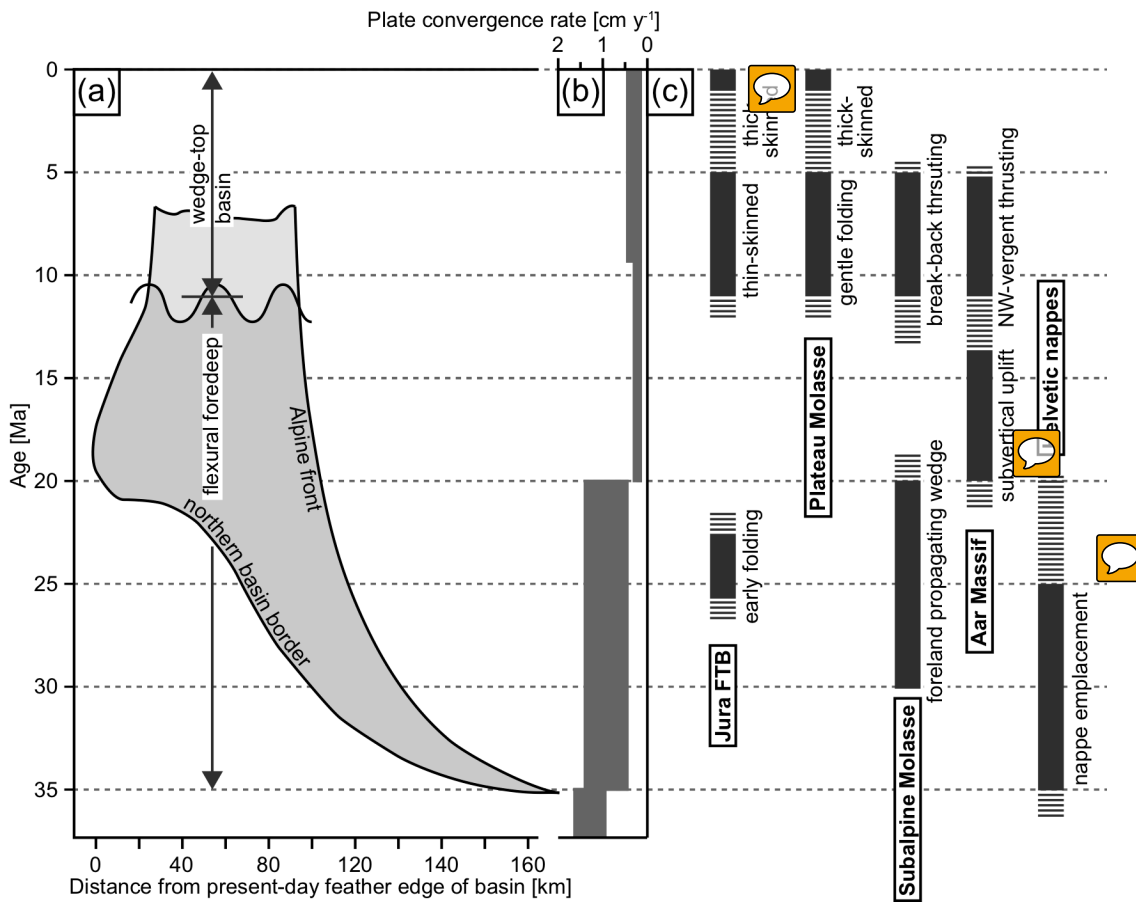
Fig. 8 Oligocene to present-day evolution of the northern Central Alps. (a) Temporal evolution of the Molasse Basin architecture (adapted from Schlunegger and Kissling, 2015). The location of the section is given in Fig. 1. (b) Rates of plate convergence between Adria and Europe (Handy et al., 2010; Schmid et al., 1996). (c) Tectonic evolution of the major tectonic units of the northern Central Alps. FTB, fold-and-thrust belt
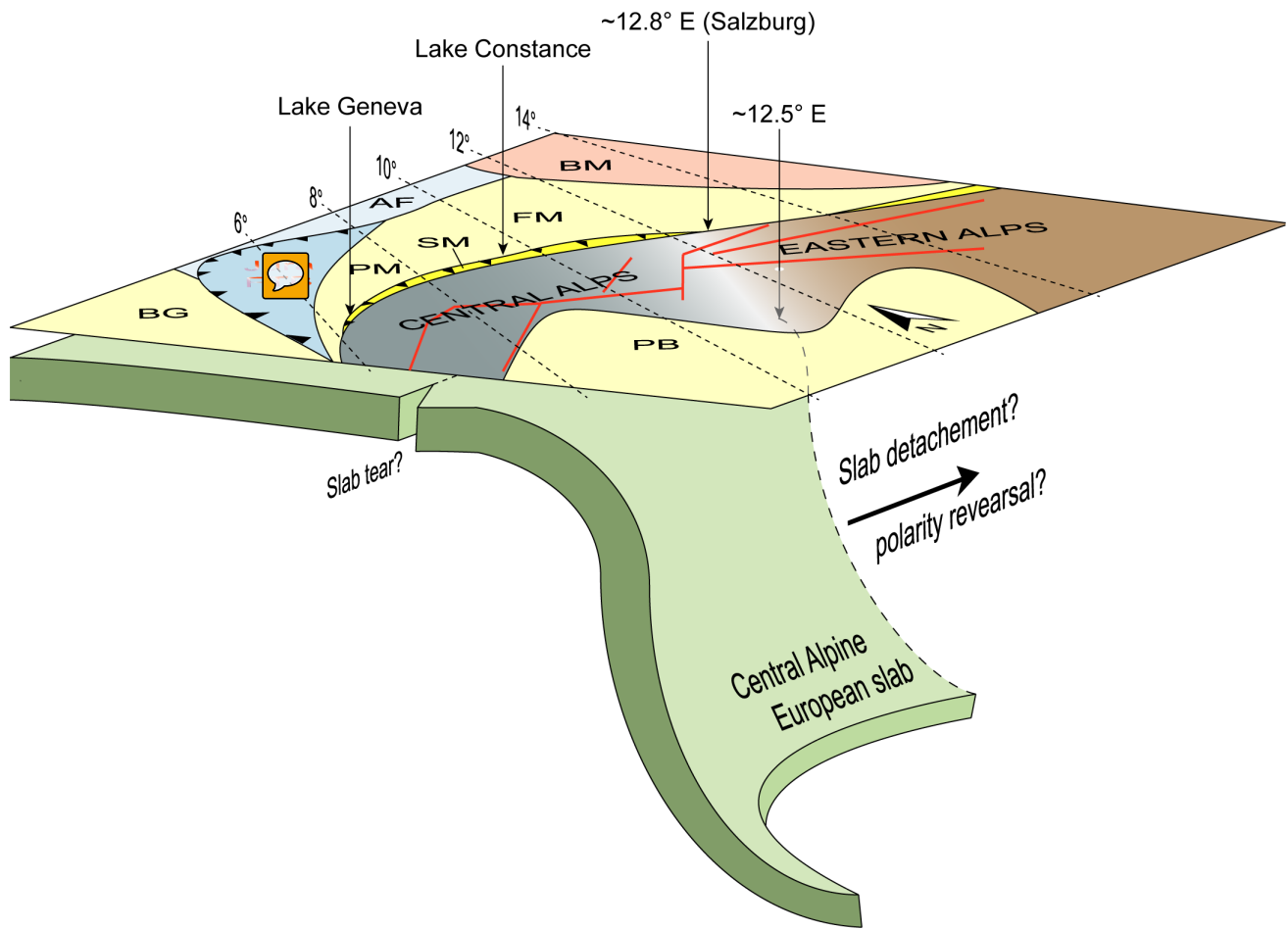
Fig. 9 Schematic 3D representation of the structure of the Central Alpine European slab and its spatial correlation with the eastward termination of the late Miocene Subalpine Molasse near Salzburg. PM, Plateau Molasse; FM, Foreland Molasse; SM, Subalpine Molasse; PB, Po Basin; TW, Tauern Window; BF, Brenner Fault; FTB, Fold-and-thrust belt; BG, Bresse Graben; AF, autochthonous foreland; BM, Bohemian Massif.